

The Higgs Boson Lineshape*

STEFANO GORIA[†], GIAMPIERO PASSARINO[‡], DARIO ROSCO[§]

*Dipartimento di Fisica Teorica, Università di Torino, Italy
INFN, Sezione di Torino, Italy*

The heavy Higgs searches at LHC are carried out in $gg \rightarrow H \rightarrow WW \rightarrow l\nu l$, $gg \rightarrow H \rightarrow ZZ \rightarrow ll ll$, $ll\nu\nu$, $llqq$ channels. The current searches for a heavy Higgs boson assume on-shell (stable) Higgs-boson production. The Higgs-boson production cross section is then sampled with a Breit-Wigner distribution (with fixed-width or running-width) and implemented in MonteCarlo simulations. Therefore the question remains of what is the limitation of the narrow Higgs-width approximation. The main focus of this work is on the description of the Standard Model Higgs-boson-lineshape in the heavy Higgs region, typically M_H above 600 GeV . The framework discussed in this paper is general enough and can be used for all processes and for all kinematical regions. Numerical results are shown for the gluon-fusion process. Issues of gauge invariance and residual theoretical uncertainties are also discussed. Limitations due to a breakdown of the perturbative expansion are comprehensively discussed, including a discussion of the equivalence theorem for (off-shell) virtual vector-bosons. Analytic continuation in a theory with unstable particles is thoroughly discussed.

Keywords: Feynman diagrams, Loop calculations, Radiative corrections, Higgs physics

PACS classification: 11.15.Bt, 12.38.Bx, 13.85.Lg, 14.80.Bn, 14.80.Cp

*Work supported by MIUR under contract 2001023713_006 and by UniTo - Compagnia di San Paolo under contract ORTO11TPXK.

[†]goria@to.infn.it

[‡]giampiero@to.infn.it

[§]rosco@to.infn.it

Contents

1	Introduction	1
2	Propagation	2
3	Production and decay	6
3.1	Schemes	9
3.2	Production cross-section	11
4	The issue of gauge invariance	12
5	Numerical results	14
5.1	Results in CPP-scheme	20
5.2	Results in the low Higgs mass region	21
6	QCD scale error	21
7	Residual theoretical uncertainty	22
7.1	Interference signal/background	25
8	Conclusions	25
A	Appendix: Nielsen identities at work	33
B	Appendix: equivalence theorem for (off-shell) virtual bosons	34
C	Appendix: complex poles, real kinematics and pseudo-observables	38
C.1	Analytic continuation	38
C.2	Pseudo-observables	43

1 Introduction

At the beginning of 2011 the status of the inclusive cross-section for Higgs-boson production in gluon fusion was summarized [1]. Corrections arising from higher-order QCD, electroweak effects, as well as contributions beyond the commonly-used effective theory approximation were analyzed. Uncertainties arising from missing terms in the perturbative expansion, as well as imprecise knowledge of parton distribution functions, were estimated to range from approximately 15–20%, with the precise value depending on the Higgs boson mass. For an updated study we refer to Ref. [2].

In this work we consider the problem of a consistent definition of the Higgs–boson-lineshape at LHC and address the question of optimal presentation of LHC data.

Some preliminary observations are needed: the Higgs system of the Standard Model has almost a non-perturbative behavior, even at a low scale. Let us consider the traditional on-shell approach and the values for the on-shell decay width of the Higgs boson [1]: for $M_H = 140 \text{ GeV}$ the total width is $8.12 \times 10^{-3} \text{ GeV}$; the process $H \rightarrow \bar{b}b$ has a partial width of $2.55 \times 10^{-3} \text{ GeV}$, other two-body decays are almost negligible while $H \rightarrow 4f$ has $4.64 \times 10^{-3} \text{ GeV}$ well below the WW -threshold. Therefore the four-body decay, even below threshold, is more important than the two-body ones. What are the corresponding implications? Since decay widths are related to the imaginary parts of loop diagrams the above statement is equivalent to say that, in terms of imaginary parts of the H self-energy, three-loop diagrams are as important as one-loop diagrams, or more.

We realize that most of the people just want to use some well-defined recipe without having to dig any deeper; however, there is no alternative to a complete description of LHC processes which has to include the complete matrix elements for all relevant processes; splitting the whole S -matrix element into components is just conventional wisdom. However, the precise tone and degree of formality must be dictated by gauge invariance.

The framework discussed in this paper is general enough and can be used for all processes and for all kinematical regions; however, the main focus of this work will be on the description of the Higgs–boson-lineshape in the heavy Higgs region, typically above 600 GeV . The general argument is well documented in the literature and, for a complete description of all technical details, we refer to Ref. [3,4]. Part of the results discussed in this paper and concerning a correct implementation of the Higgs–boson-lineshape have been summarized in a talk at the BNL meeting of the HXSWG¹. It is important to stress the exact content of this work: we deal with a gauge invariant definition of the signal, which assumes that the non-resonant background and the signal/background interference have been subtracted from the data.

One might wonder why considering a Standard Model (SM) Higgs boson in such a high-mass range. There are classic constraints on the Higgs boson mass coming from unitarity, triviality and vacuum stability, precision electroweak data and absence of fine-tuning [5]. However, the search for a SM Higgs boson over a mass range from 80 GeV to 1 TeV is clearly indicated as a priority in many experimental papers, e.g. *ATLAS: letter of intent for a general-purpose pp experiment at the large hadron collider at CERN*². For recent results, see Ref. [6,7,8,9,10,11,12].

The situation is different if we consider extensions of the SM: in the two Higgs doublet (THD) model, even if the SM-like Higgs boson is found to be light ($< 140 \text{ GeV}$), there is a possible range of mass splitting in the heavy Higgs boson. In general, for a given Higgs boson mass, the magnitude of the mass splittings among different heavy scalar bosons can be determined to satisfy the electroweak precision data, see Ref. [13].

In addition, the work of Ref. [14] studies scenarios where a heavy Higgs boson can be made consistent with both the indirect constraints and the direct null searches by adding only one new particle beyond the Standard Model. Heavy Higgs effects in a theory with a fourth Standard-Model-like fermion generation have been examined in Refs. [15,16].

The work of Ref. [17] critically reviews models that allow a heavy Higgs boson consistent with the precision electroweak constraints. All have unusual features, and all can be distinguished from the Minimal SM either by improved precision measurements or by other signatures accessible to next-generation colliders.

¹<http://www.bnl.gov/hcs/>

²<http://atlas.web.cern.ch/Atlas/internal/tdr.html>

Coming back to the framework that we are introducing, there is another important issue: when working in the on-shell scheme one finds that the two-loop corrections to the on-shell Higgs width exceed the one-loop corrections if the on-shell Higgs mass is larger than 900 GeV , as discussed in Ref. [18]. This fact simply tells you that perturbation theory diverges badly, starting from approximately 1 TeV . In this work we will also illustrate the corresponding impact on the Higgs boson lineshape (previous work can be found in Refs. [19,20]).

Recently the problem of going beyond the zero-width approximation has received new boost from the work of Refs. [21,22]: the program iHIXS allow the study of the Higgs–boson-lineshape for a finite width of the Higgs boson and computes the cross-section sampling over a Breit-Wigner distribution. There is, however, a point that has been ignored in all calculations performed so far: the Higgs boson is an unstable particle and should be removed from the in/out bases in the Hilbert space, without destroying the unitarity of the theory. Therefore, concepts as the *production* of an unstable particle or its *partial decay widths* do not have a precise meaning and should be replaced by a conventionalized definition which respects first principles of Quantum Field Theory (QFT).

This paper is organized as follows. In Section 2 we introduce and discuss complex poles for unstable particles. In Section 3 we analyze production and decay of a Higgs boson at LHC. A discussion on gauge invariance is presented in Section 4. In Section 6 we present a short discussion on the QCD scale error. In Section 5 we present numerical results while in Section 7 we discuss the residual theoretical uncertainty. Finally, technical details are discussed in Appendices, in particular in Appendix B we discuss how to apply the equivalence theorem for virtual vector-bosons and in Appendix C.1 we discuss analytic continuation in a theory with unstable particles.

2 Propagation

To start our discussion we consider the process $ij \rightarrow \text{H}(\rightarrow \text{F}) + \text{X}$ where $i, j \in \text{partons}$ and F is a generic final state (e.g. $\text{F} = \gamma\gamma, 4\text{f}$, etc.). For the sake of simplicity we neglect, for a moment, folding the partonic process with parton distribution functions (PDFs). Since the Higgs boson is a scalar resonance we can split the whole process into three parts, *production*, *propagation* and *decay*. In QFT all amplitudes are made out of propagators and vertices and the (Dyson-resummed) propagator for the Higgs boson reads as follows:

$$\Delta_{\text{H}}(s) = \left[s - M_{\text{H}}^2 + S_{\text{HH}} \left(s, M_{\text{t}}^2, M_{\text{H}}^2, M_{\text{W}}^2, M_{\text{Z}}^2 \right) \right]^{-1}, \quad (1)$$

where M_i is a renormalized mass and S_{HH} is the renormalized Higgs self-energy (to all orders but with one-particle-irreducible diagrams). The first argument of the self-energy in Eq.(1) is the external momentum squared, the remaining ones are (renormalized) masses in the loops. We define complex poles for unstable particles as the (complex) solutions of the following system:

$$\begin{aligned} s_{\text{H}} - M_{\text{H}}^2 + S_{\text{HH}} \left(s_{\text{H}}, M_{\text{t}}^2, M_{\text{H}}^2, M_{\text{W}}^2, M_{\text{Z}}^2 \right) &= 0, \\ s_{\text{W}} - M_{\text{W}}^2 + S_{\text{WW}} \left(s_{\text{W}}, M_{\text{t}}^2, M_{\text{H}}^2, M_{\text{W}}^2, M_{\text{Z}}^2 \right) &= 0, \end{aligned} \quad (2)$$

etc. To lowest order accuracy the Higgs propagator can be rewritten as

$$\Delta_{\text{H}}^{-1} = s - s_{\text{H}}. \quad (3)$$

The complex pole describing an unstable particle is conventionally parametrized as

$$s_i = \mu_i^2 - i \mu_i \gamma_i, \quad (4)$$

where μ_i is an input parameter (similar to the on-shell mass) while γ_i can be computed (as the on-shell total width), say within the Standard Model. There are other, equivalent, parametrizations [18], e.g. $\sqrt{s_{\text{H}}} = \mu_{\text{H}} - i/2 \gamma_{\text{H}}$. Note that the the pole of Δ fully embodies the propagation properties of a particle. We know

that even in ordinary Quantum Mechanics the resonances are described as the complex energy poles in the scattering amplitude. The general formalism for describing unstable particles in QFT was developed long ago, see Refs. [23,24,25,26,27]; for an implementation in gauge theories we refer to the work of Refs. [28,29,30,31], for complex poles in general to Refs. [32,33,34] and Refs. [35,36]. For alternative approaches we refer to the work of Refs. [37,38].

We can summarize by saying that unstable particles are described by irreducible, nonunitary representations of the Poincare group, corresponding to the complex eigenvalues of the four-momentum p^μ satisfying the condition $p^2 = -\mu^2 + i\mu\gamma$. For a discussion on violation of the spectral condition we refer to Ref. [39].

Consider the complex mass scheme (CMS) introduced in Ref. [40,41] (see also Ref. [42]) and extended at two-loop level in Ref. [43]: here, at lowest level of accuracy, we use

$$s_H - M_H^2 + S_{HH}(s_H, s_t, s_H, s_W, s_Z) = 0, \quad (5)$$

where now S_{HH} is computed at one loop level and s_W etc. are the experimental complex poles, derived from the corresponding (experimental) on-shell masses and widths. For the W and Z bosons the input parameter set (IPS) is defined in terms of pseudo-observables; at first, on-shell pseudo-quantities are derived by fitting the experimental lineshapes with

$$\Sigma_{VV}(s) = \frac{N}{(s - M_{OS}^2)^2 + s^2 \Gamma_{OS}^2 / M_{OS}^2}, \quad V = W, Z, \quad (6)$$

where N is an irrelevant (for our purposes) normalization constant. Secondly, we define pseudo-observables

$$M_P = M_{OS} \cos \psi, \quad \Gamma_P = \Gamma_{OS} \sin \psi, \quad \psi = \arctan \frac{\Gamma_{OS}}{M_{OS}}, \quad (7)$$

which are inserted in the IPS. Renormalization with complex poles should not be confused with a simple recipe for the replacement of running widths with constant widths; there are many more ingredients in the scheme. It is worth noting that perturbation theory based on s_H instead of the on-shell mass has much better convergence properties; indeed, as shown in Ref. [18], the two-loop corrections to the imaginary part of s_H become as large as the one-loop ones *only* when $\mu_H = 1.74 TeV$. This suggests that the complex pole scheme is preferable also from the point of view of describing the heavy Higgs-boson production at LHC.

There is a substantial difference between W,Z complex poles and the Higgs complex pole. In the first case W,Z bosons decay predominantly into two (massless) fermions while for the Higgs boson below the WW-threshold the decay into four fermions is even larger than the decay into a $\bar{b}b$ pair, while the other fermion pairs are heavily suppressed by vanishing Yukawa couplings. Therefore we cannot use for the Higgs boson the well-known result,

$$\text{Im } S_{VV}(s) \approx \frac{\Gamma_V^{OS}}{M_V^{OS}} s. \quad (8)$$

which is valid for W,Z. As a consequence of this fact we have

$$\mu_V^2 = M_{VOS}^2 - \Gamma_{VOS}^2 + \text{HO}, \quad \gamma_V = \Gamma_V^{OS} \left[1 - \frac{1}{2} \left(\frac{\Gamma_V^{OS}}{M_V^{OS}} \right)^2 \right] + \text{HO}, \quad (9)$$

where the perturbative expansion is well under control since $\Gamma_V^{OS}/M_V^{OS} \ll 1$. For the Higgs boson we have a different expansion,

$$\begin{aligned} \gamma_H &= \Gamma_H \left[1 + \sum_n a_n \Gamma_H^n \right] + \sum_{V=W,Z} \frac{M_V}{M_H} \sum_{n,l} b_{nl}^V \Gamma_V^n \Gamma_H^l, \\ a_0 &= -[\text{Im } S_{HH,OS}^h]^2, \quad a_1 = \frac{1}{2} \left[\frac{1}{M_H} \text{Im } S_{HH,OS}^h - M_H \text{Im } S_{HH,OS}^{hh} \right], \\ b_{10}^V &= -\text{Re } S_{HH,OS}^v + \text{Re } S_{HH,OS}^v \text{Re } S_{HH,OS}^h - \text{Im } S_{HH,OS}^v \text{Im } S_{HH,OS}^h \end{aligned}$$

$$b_{11}^V = \frac{1}{2 M_H} \text{Im } S_{\text{HH}, \text{OS}}^v - M_H \text{Im } S_{\text{HH}, \text{OS}}^{hv}, \quad b_{20}^V = -\frac{1}{2} \frac{M_V}{M_H} \text{Im } S_{\text{HH}, \text{OS}}^{vv} \quad (10)$$

Here we have $M_i = M_i^{\text{OS}}$, $\Gamma_i = \Gamma_i^{\text{OS}}$ (on-shell quantities) and

$$S_{\text{HH}, \text{OS}}^{a_1 \dots a_n} = \frac{\partial^n}{\partial M_{a_1}^2 \dots \partial M_{a_n}^2} S_{\text{HH}} \left(M_H^2, M_t^2, M_H^2, M_W^2, M_Z^2 \right), \quad (11)$$

where only the first few terms in the perturbative expansion are explicitly given. In Eq.(10) we used the following definition of the on-shell width

$$\Gamma_H^{\text{OS}} M_H^{\text{OS}} = \text{Im } S_{\text{HH}, \text{OS}} + \text{HO} \quad (12)$$

Only the complex pole is gauge-parameter independent to all orders of perturbation theory while on-shell quantities are ill-defined beyond lowest order. Indeed, in the R_ξ gauge, at lowest order, one has the following expression for the bosonic part of the Higgs self-energy:

$$\text{Im } S_{\text{HH}, \text{bos}}(s) = \frac{g^2}{4 M_W^2} s^2 \left[\left(\frac{M_H^4}{s^2} - 1 \right) \left(1 - 4 \xi_W \frac{M_W^2}{s} \right)^{1/2} \theta \left(s - 4 \xi_W M_W^2 \right) + \frac{1}{2} (W \rightarrow Z) \right], \quad (13)$$

where ξ_V ($V = W, Z$) are gauge parameters. Note that Eq.(10) (the expansion) involves derivatives.

Starting from Eq.(13) we understand the problem with the on-shell definition of the mass: once again, let M_H be the renormalized Higgs mass and $s_H = \mu_H^2 - i \mu_H \gamma_H$ the parametrization of the complex pole; it follows

$$\begin{aligned} M_H^2 |_{\text{OS}} &= M_H^2 + \text{Re } S_{\text{HH}}(M_H^2), & \mu_H^2 &= M_H^2 + \text{Re } S_{\text{HH}}(s_H), \\ M_H |_{\text{OS}} - \mu_H &= -\frac{1}{2} \gamma_H \text{Im } S'_{\text{HH}}(\mu_H^2), \end{aligned} \quad (14)$$

showing that at order g^4 the on-shell mass is ill-defined since s_H is ξ -independent.

A technical remark: suppose that we use μ_H as a *free* input parameter and derive γ_H in the SM from the equation

$$\mu_H \gamma_H = \text{Im } S_{\text{HH}}(s_H, s_t, s_H, s_W, s_Z). \quad (15)$$

Since the bare W, Z masses are replaced with complex poles also in couplings (to preserve gauge invariance) it follows that γ_H (solution of Eq.(15)) is renormalization scale dependent; while counterterms can be introduced to make the self-energy ultraviolet finite, the μ_R dependence drops only in subtracted quantities, i.e. after finite renormalization, something that would require knowledge of the experimental Higgs complex pole [44,43]. Following our intuition we fix the scale at $\mu_R = \mu_H$.

After evaluating the coefficients of Eq.(10) (e.g. in the $\xi = 1$ gauge) it is easily seen that the expanded solution of Eq.(5) is not a good approximation to exact one, especially for high values of μ_H . For instance, for $\mu_H = 500 \text{ GeV}$ we have an exact solution $\gamma_H = 58.70 \text{ GeV}$, an expanded one of 62.87 GeV with an on-shell width of 68.0 GeV . Therefore, we will use an exact, numerical, solution for γ_H ; details on the structure of the Higgs self-energy to all orders of perturbation theory can be found in Ref. [44,43].

It is important to remark that an evaluation of γ_H at the same level of accuracy to which Γ_H^{OS} is known (see Ref. [1]) would require, at least, a three-loop calculation (the first instance where we have a four-fermion cut of the H self-energy).

Complex poles for unstable W, Z, H and t also tell us that it is very difficult for an heavy Higgs boson to come out right within the SM; these complex poles are solutions of a (coupled) system of equations but for W, Z and (partially) t we can compare with the corresponding experimental quantities. Results are shown in Table 1 and clearly indicate mismatches between predicted and experimental W, t complex poles. Indeed, as soon as μ_H increases, it becomes more and more difficult to find complex W, t and Z poles with an imaginary part compatible with measurements.

Table 1: The Higgs boson complex pole at fixed values of the W, t complex poles compared with the complete solution for s_H, s_W and s_t

μ_H [GeV]	γ_W [GeV] fixed	γ_t [GeV] fixed	γ_H [GeV] derived
200	2.088	1.481	1.355
250			3.865
300			8.137
350			14.886
400			26.598
μ_H [GeV]	γ_W [GeV] derived	γ_t [GeV] derived	γ_H [GeV] derived
200	2.130	1.085	1.356
250	2.119	0.962	3.823
300	2.193	0.836	8.139
350	2.607	0.711	14.653
400	3.922	0.566	25.498

This simple fact raises the following question: what is the physical meaning of an heavy Higgs boson search? We have the usual and well-known considerations [5]: a Higgs boson above 600 GeV requires new physics at 1 TeV , argument based on partial-wave unitarity [45,46] (which should not be taken quantitatively or too literally); violation of unitarity bound possibly implies the presence of $J = 0, 1$ resonances but there is no way to predict their masses, simply scaling the $\pi-\pi$ system gives resonances in the 1 TeV range. Generally speaking, it would be a good idea to address this search as *search* for $J = 0, 1$ heavy resonances decaying into $VV \rightarrow 4f$. In a model independent approach both μ_H and γ_H should be kept free in order to perform a 2 dim scan of the Higgs-boson lineshape. For the high-mass region this remains our recommended strategy. Once the fits are performed it will be left to theorists to struggle with a model-dependent interpretation of the results.

To summarize, we have addressed the following question: what is the common sense definition of mass and width of the Higgs boson? We have several options,

$$s_H = \mu_H^2 - i \mu_H \gamma_H, \quad s_H = \left(\mu'_H - \frac{i}{2} \gamma'_H \right)^2, \quad s_H = \frac{\overline{M}_H^2 - i \overline{\Gamma}_H \overline{M}_H}{1 + \overline{\Gamma}_H^2 / \overline{M}_H^2}. \quad (16)$$

We may ask which one is correct, approximate or closer to the experimental peak. Here we have to distinguish: for $\gamma_H \ll \mu_H$ \overline{M}_H is a good approximation to the on-shell mass and it is closer to the experimental peak; for instance, for the Z boson \overline{M}_Z is equivalent to the mass measured at Lep. However, in the high-mass scenario, where $\gamma_H \sim \mu_H$, the situation changes an $\overline{O}_H \neq O_H^{OS}$ for any observable (or pseudo-observable). Therefore, the message is: do not use the on-shell width to estimate \overline{M}_H in the high-mass region.

Missing a calculation of the three-loop Higgs self-energy we can analyze the low-mass region by using an approximation to the exact Higgs complex-pole which is based on the expansion of γ_H around the best-known on-shell calculation, Γ_p from PROPHECY4F [47]. Therefore, below $\mu_H = 200$ GeV we will use

$$\frac{\gamma_H}{\Gamma_p} \approx 1 + \frac{1}{2} X_W \left(d_1 - \mu_H^2 d_2 \right) \frac{\Gamma_p}{\mu_H} - X_W^2 d_1^2, \quad (17)$$

$$X_W = 4 \sqrt{2} \frac{G_F M_W^2}{\pi^2}, \quad d_n = \frac{\partial^n}{\partial \mu_H^n} S_{HH}. \quad (18)$$

In the expansion all masses but the Higgs mass are kept real and the higher-order effects are simulated by the expansion parameter, Γ_p / μ_H .

3 Production and decay

Before describing production and decay of an Higgs boson we underline the general structure of any process containing a Higgs boson intermediate state. The corresponding amplitude is schematically given by

$$A(s) = \frac{f(s)}{s - s_H} + N(s), \quad (19)$$

where $N(s)$ denotes the part of the amplitude which is non-Higgs-resonant. Signal (S) and background (B) are defined as follows:

$$A(s) = S(s) + B(s), \quad S(s) = \frac{f(s_H)}{s - s_H}, \quad B(s) = \frac{f(s) - f(s_H)}{s - s_H} + N(s). \quad (20)$$

As a first step we will show how to write $f(s)$ in a way such that pseudo-observables make their appearance. Consider the process $ij \rightarrow H \rightarrow F$ where $i, j \in \text{partons}$ and F is a generic final state; the complete cross-section will be written as follows:

$$\sigma_{ij \rightarrow H \rightarrow F}(s) = \frac{1}{2s} \int d\Phi_{ij \rightarrow F} \left[\sum_{s,c} |A_{ij \rightarrow H}|^2 \right] \frac{1}{|s - s_H|^2} \left[\sum_{s,c} |A_{H \rightarrow F}|^2 \right], \quad (21)$$

where $\sum_{s,c}$ is over spin and colors (averaging on the initial state). Note that the background (e.g. $gg \rightarrow 4f$, see Ref. [48,49,50]) has not been included and, strictly speaking and for reasons of gauge invariance, one should consider only the residue of the Higgs-resonant amplitude at the complex pole, as described in Eq.(20). For the moment we will argue that the dominant corrections are the QCD ones where we have no problem of gauge parameter dependence. If we decide to keep the Higgs boson off-shell also in the resonant part of the amplitude (interference signal/background remains unaddressed) then we can write

$$\int d\Phi_{ij \rightarrow H} \sum_{s,c} |A_{ij \rightarrow H}|^2 = s \bar{A}_{ij}(s). \quad (22)$$

For instance, we have

$$\bar{A}_{gg}(s) = \frac{\alpha_s^2}{\pi^2} \frac{G_F s}{288 \sqrt{2}} \left| \sum_q f(\tau_q) \right|^2 (1 + \delta_{\text{QCD}}), \quad (23)$$

where $\tau_q = 4m_q^2/s$, $f(\tau_q)$ is defined in Eq.(3) of Ref. [51] and where δ_{QCD} gives the QCD corrections to $gg \rightarrow H$ up to next-to-next-to-leading-order (NNLO) + next-to-leading logarithms (NLL) resummation. Furthermore, we define

$$\Gamma_{H \rightarrow F}(s) = \frac{1}{2\sqrt{s}} \int d\Phi_{H \rightarrow F} \sum_{s,c} |A_{H \rightarrow F}|^2, \quad (24)$$

which gives the partial decay width of a Higgs boson of virtuality s into a final state F .

$$\sigma_{ij \rightarrow H} = \frac{\bar{A}_{ij}(s)}{s}, \quad (25)$$

which gives the production cross-section of a Higgs boson of virtuality s . We can write the final result in terms of pseudo-observables

$$\sigma_{ij \rightarrow H \rightarrow F}(s) = \frac{1}{\pi} \sigma_{ij \rightarrow H} \frac{s^2}{|s - s_H|^2} \frac{\Gamma_{H \rightarrow F}}{\sqrt{s}}. \quad (26)$$

It is also convenient to rewrite the result as

$$\sigma_{ij \rightarrow H \rightarrow F}(s) = \frac{1}{\pi} \sigma_{ij \rightarrow H} \frac{s^2}{|s - s_H|^2} \frac{\Gamma_H^{\text{tot}}}{\sqrt{s}} \text{BR}(H \rightarrow F), \quad (27)$$

where we have introduced a sum over all final states,

$$\Gamma_{\text{H}}^{\text{tot}} = \sum_{f \in \text{F}} \Gamma_{\text{H} \rightarrow \text{F}}. \quad (28)$$

Note that we have written the phase-space integral for $i(p_1) + j(p_2) \rightarrow \text{F}$ as

$$\int d\Phi_{ij \rightarrow \text{F}} = \int d^4k \delta^4(k - p_1 - p_2) \int \prod_f d^4p_f \delta^+(p_f^2) \delta^4(k - \sum_f p_f), \quad (29)$$

where we assume that all initial and final states (e.g. $\gamma\gamma$, $4f$, etc.) are massless.

It is worth noting that the introduction of complex poles does not imply complex kinematics. According to Eq.(20) only the residue of the propagator at the complex pole becomes complex, not any element of the phase-space integral. Details of the procedure are discussed in Appendix C.

On a more formal bases one should say that unstable states lie in a natural extension of the usual Hilbert space that corresponds to the second sheet of the S -matrix; these states have zero norm and, therefore, escape the usual prohibition of having an hermitian Hamiltonian with complex energy [52]. On a more pragmatic level we use the guiding principle that Green's functions involving unstable particles should smoothly approach the value for stable ones (the usual Feynman $-i0$ prescription) when the couplings of the theory tend to zero.

If we insist that $|\text{H}\rangle$ is an asymptotic state in the Hilbert space then the observable to consider will be $\langle \text{F out} | \text{H in} \rangle$, otherwise one should realize that for stable particles the proof of the LSZ reduction formulas [53] depends on the existence of asymptotic states

$$|p \text{ in} \rangle = \lim_{t \rightarrow -\infty} \int d^3x H(x) i \overleftrightarrow{\partial}_t e^{i p \cdot x} |0 \rangle, \quad (30)$$

(in the weak operator sense). For unstable particles the energy is complex so that this limit either diverges or vanishes. Although a modification of the LSZ reduction formulas has been proposed long ago for unstable particles, see Ref. [52], we prefer an alternative approach where one considers extracting information on the Higgs boson directly from

$$\langle \text{F out} | \text{H} \rangle \langle \text{H} | \text{I in} \rangle + \sum_{n \neq \text{H}} \langle \text{F out} | n \rangle \langle n | \text{I in} \rangle, \quad (31)$$

for some initial state I and some final state F and where $\{n\} \oplus \text{H}$ is a complete set of states (not as in the in/out bases). As we have seen, the price to be paid is the necessity of moving into the complex plane. Why do we need pseudo-observables? Ideally experimenters (should) extract so-called *realistic observables* from raw data, e.g. $\sigma(\text{pp} \rightarrow \gamma\gamma + \text{X})$ and (should) present results in a form that can be useful for comparing them with theoretical predictions, i.e. the results should be transformed into pseudo-observables; during the deconvolution procedure one should also account for the interference background – signal; theorists (should) compute pseudo-observables using the best available technology and satisfying a list of demands from the self-consistency of the underlying theory.

- **Definition** We define an off-shell production cross-section (for all channels) as follows:

$$\sigma_{ij \rightarrow \text{all}}^{\text{prop}} = \frac{1}{\pi} \sigma_{ij \rightarrow \text{H}} \frac{s^2}{|s - s_{\text{H}}|^2} \frac{\Gamma_{\text{H}}^{\text{tot}}}{\sqrt{s}}. \quad (32)$$

When the cross-section $ij \rightarrow \text{H}$ refers to an off-shell Higgs boson the choice of the QCD scales should be made according to the virtuality and not to a fixed value. Therefore, always referring to Figure 9, for the PDFs and $\sigma_{ij \rightarrow \text{H} + \text{X}}$ one should select $\mu_{\text{F}}^2 = \mu_{\text{R}}^2 = z s/4$ ($z s$ being the invariant mass of the detectable final state). Indeed, beyond lowest order (LO) one must not choose the invariant mass of the incoming partons for the renormalization and factorization scales, with the factor 1/2 motivated by an improved convergency of

fixed order expansion, but an infrared safe quantity fixed from the detectable final state, see Ref. [54]. The argument is based on minimization of the universal logarithms (DGLAP) and not the process-dependent ones³.

The off-shell Higgs-boson production is currently computed according to the replacement

$$\sigma_{\text{OS}}(\mu_{\text{H}}^2) \delta(\zeta - \mu_{\text{H}}^2) \implies \sigma_{\text{OFS}}(\zeta) \text{BW}(\zeta), \quad (33)$$

(e.g. see Ref. [55]) at least at lowest QCD order, where the so-called modified Breit–Wigner distribution is defined by

$$\text{BW}(s) = \frac{1}{\pi} \frac{s \Gamma_{\text{H}}^{\text{OS}} / \mu_{\text{H}}}{\left(s - \mu_{\text{H}}^2\right)^2 + \left(s \Gamma_{\text{H}}^{\text{OS}} / \mu_{\text{H}}\right)^2}, \quad (34)$$

where now $\mu_{\text{H}} = M_{\text{H}}^{\text{OS}}$ and $\zeta = z s$. This ad-hoc Breit–Wigner cannot be derived from QFT and also is not normalizable in $[0, +\infty]$. Note that this Breit–Wigner for a running width comes from the substitution of $\Gamma \rightarrow \Gamma(s) = \Gamma s / M^2$ in the Breit–Wigner for a fixed width Γ . This substitution is not justifiable. Its practical purpose is to enforce a *physical* behavior for low virtualities of the Higgs boson but the usage cannot be justified or recommended. For instance, if one considers VV scattering and uses this distribution in the s -channel Higgs exchange, the behavior for large values of s spoils unitarity cancellation with the contact diagram. It is worth noting that the alternative replacement

$$\sigma_{\text{OS}}(\mu_{\text{H}}^2) \delta(\zeta - \mu_{\text{H}}^2) \implies \sigma_{\text{OFS}}(\zeta) \text{BW}(\zeta), \quad \text{BW}(\zeta) = \frac{1}{\pi} \frac{\mu_{\text{H}} \Gamma_{\text{H}}^{\text{OS}}}{\left(\zeta - \mu_{\text{H}}^2\right)^2 + \left(\mu_{\text{H}} \Gamma_{\text{H}}^{\text{OS}}\right)^2}, \quad (35)$$

has additional problems at the low energy tail of the resonance due to the gg -luminosity, creating an artificial increase of the lineshape at low virtualities⁴.

Another important issue is that γ_{H} which appears in the imaginary part of the inverse Dyson-resummed propagator is not the on-shell width since they differ by higher-order terms and their relations becomes non-perturbative when the on-shell width becomes of the same order of the on-shell mass (typically, for on-shell masses above 800 GeV). For nonlinear parameterizations of the scalar sector of the standard model and Dyson summation of the Higgs self energy we refer to the work of Ref. [56].

The complex-mass scheme can be translated into a more familiar language by introducing the Bar-scheme. Using Eq.(3) with the parametrization of Eq.(4) we perform the well-known transformation

$$\overline{M}_{\text{H}}^2 = \mu_{\text{H}}^2 + \gamma_{\text{H}}^2 \quad \mu_{\text{H}} \overline{\Gamma}_{\text{H}} = \overline{M}_{\text{H}} \gamma_{\text{H}}. \quad (36)$$

A remarkable identity follows (defining the Bar-scheme):

$$\frac{1}{s - s_{\text{H}}} = \left(1 + i \frac{\overline{\Gamma}_{\text{H}}}{\overline{M}_{\text{H}}}\right) \left(s - \overline{M}_{\text{H}}^2 + i \frac{\overline{\Gamma}_{\text{H}}}{\overline{M}_{\text{H}}} s\right)^{-1}, \quad (37)$$

showing that the Bar-scheme is equivalent to introducing a running width in the propagator with parameters that are not the on-shell ones. Special attention goes to the numerator in Eq.(37) which is essential in providing the right asymptotic behavior when $s \rightarrow \infty$, as needed for cancellations with contact terms in VV scattering. If we compare the result of Eq.(37) with Eq.(4) of Ref. [57] and interpret m_{H} and Γ_{H} of that equation as the corresponding Bar - scheme quantities \overline{M}_{H} and $\overline{\Gamma}_{\text{H}}$ of Eq.(36), we see that the so-called Seymour - scheme of Refs. [21,22] is exactly giving the Higgs propagator with a complex pole. There is a second variant for the Higgs propagator in Ref. [57], i.e. (in the notation of that paper)

$$\Delta_{\text{H}}(s) = \frac{m_{\text{H}}^2}{s} \left[s - m_{\text{H}}^2 + i \frac{\Gamma_{\text{H}}}{m_{\text{H}}} s\right]^{-1} \quad (38)$$

³We gratefully acknowledge S. Forte and M. Spira for an important discussion on this point.

⁴We gratefully acknowledge S. Frixione for an important discussion on this point.

Table 2: Higgs boson complex pole; $\Gamma_{\text{H}}^{\text{OS}}$ is the on-shell width, γ_{H} is defined in Eq.(4) and the Bar-scheme in Eq.(36).

$\mu_{\text{H}}[\text{GeV}]$	$\Gamma_{\text{H}}^{\text{OS}}[\text{GeV}]$ (Ref. [1])	$\gamma_{\text{H}} [\text{GeV}]$	$\overline{M}_{\text{H}}[\text{GeV}]$	$\overline{\Gamma}_{\text{H}}[\text{GeV}]$
200	1.43	1.35	200	1.35
400	29.2	25.60	400.9	26.66
600	123	103.93	608.9	105.48
700	199	162.97	718.7	167.33
800	304	235.57	834.0	245.57
900	449	320.55	955.4	340.28
1000	647	416.12	1083.1	450.71

which has been used afterwards with the motivation that the prescription accounts for signal-background interference effects. If we denote by A_{H} the Higgs-resonant amplitude and by A_{B} the box contribution in $gg \rightarrow ZZ$ then the interference is

$$A_{\text{int}} = 2 \text{Re} (\Delta_{\text{H}} I^{\dagger}), \quad I = \overline{A}_{\text{H}} A_{\text{B}}^{\dagger}, \quad \overline{A}_{\text{H}} = (s - s_{\text{H}}) A_{\text{H}}. \quad (39)$$

Note that for large values of the Higgs mass the term in Eq.(39) proportional to $\text{Im} \Delta_{\text{H}}$ is not negligible. The main issue in Ref. [57] is on unitarity cancellations at high energy. Of course, the behavior of both amplitudes for $s \rightarrow \infty$ is known and simple and any correct treatment of perturbation theory (no mixing of different orders) will respect the unitarity cancellations; from this point of view, the numerator in Eq.(37) is essential. Since the Higgs boson decays almost completely into longitudinal Zs, for $s \rightarrow \infty$ we have [58] (for a single quark q)

$$A_{\text{H}} \sim \frac{sm_q^2}{2M_Z^2} \Delta_{\text{H}} \ln^2 \frac{s}{m_q^2} \quad A_{\text{B}} \sim -\frac{m_q^2}{2M_Z^2} \ln^2 \frac{s}{m_q^2} \quad (40)$$

showing cancellation in the limit ($s \Delta_{\text{H}} \rightarrow 1$). However, the behavior for $s \rightarrow \infty$ (unitarity) should not/cannot be used to simulate the interference for $s < M_{\text{H}}^2$. The only relevant message to be derived here is that unitarity requires the interference to be destructive at large values of s , see also Ref. [59].

A sample of numerical results is shown in Table 2 where we compare the Higgs boson complex pole to the corresponding quantities in the Bar-scheme.

In conclusion, the use of the complex pole is recommended even if the accuracy at which its imaginary part can be computed is not of the same quality as the next-to-leading-order (NLO) accuracy of the on-shell width. Nevertheless, the use of a solid prediction (from a theoretical point of view) should always be preferred to the introduction of ill-defined quantities (lack of gauge invariance).

3.1 Schemes

We are now in a position to give a more detailed description of the strategy behind Eq.(20). Consider the complete amplitude for a given process, e.g. the one in Figure 9; let $(\zeta = zs, \dots)$ the the full list of Mandelstam invariants characterizing the process, then

$$A(\zeta, \dots) = V_{\text{prod}}(\zeta, \dots) \Delta_{\text{prop}}(\zeta) V_{\text{dec}}(\zeta) + N(\zeta, \dots). \quad (41)$$

Here V_{prod} denotes the amplitude for production, e.g. $gg \rightarrow \text{H}(\zeta) + \text{X}$, $\Delta_{\text{prop}}(\zeta)$ is the propagation function, $V_{\text{dec}}(\zeta)$ is the amplitude for decay, e.g. $\text{H}(\zeta) \rightarrow 4\text{f}$. If no attempt is made to split $A(s)$ no ambiguity arises but, usually, the two components are known at different orders. Ho to define the signal? The following schemes are available:

ONBW

$$S(\zeta, \dots) = V_{\text{prod}}(\mu_{\text{H}}^2, \dots) \Delta_{\text{prop}}(\zeta) V_{\text{dec}}(\mu_{\text{H}}^2) \quad \Delta_{\text{prop}}(\zeta) = \text{Breit-Wigner}. \quad (42)$$

in general violates gauge invariance, neglects the Higgs off-shellness and introduces the ad hoc Breit-Wigner of Eq.(34).

OFFBW

$$S(\zeta, \dots) = V_{\text{prod}}(\zeta, \dots) \Delta_{\text{prop}}(\zeta) V_{\text{dec}}(\zeta), \quad \Delta_{\text{prop}}(\zeta) = \text{Breit-Wigner}, \quad (43)$$

in general violates gauge invariance, and introduces an ad hoc Breit-Wigner.

ONP

$$S(\zeta, \dots) = V_{\text{prod}}(\mu_{\text{H}}^2, \dots) \Delta_{\text{prop}}(\zeta) V_{\text{dec}}(\mu_{\text{H}}^2), \quad \Delta_{\text{prop}}(\zeta) = \text{propagator} \quad (44)$$

in general violates gauge invariance and neglects the Higgs off-shellness.

OFFP

$$S(\zeta, \dots) = V_{\text{prod}}(\zeta, \dots) \Delta_{\text{prop}}(\zeta) V_{\text{dec}}(\zeta), \quad \Delta_{\text{prop}}(\zeta) = \text{propagator}, \quad (45)$$

in general violates gauge invariance

CPP

$$S(\zeta, \dots) = V_{\text{prod}}(s_{\text{H}}, \dots) \Delta_{\text{prop}}(\zeta) V_{\text{dec}}(s_{\text{H}}), \quad \Delta_{\text{prop}}(\zeta) = \text{propagator}. \quad (46)$$

This scheme respects all requirements: only the pole, the residue and the remainder of $A(\zeta)$ are gauge invariant. Furthermore the CPP-scheme allows to identify POs like the production cross-section and any partial decay width by putting in one-to-one correspondence robust theoretical quantities and experimental data.

From the list above it follows that only CPP-scheme should be used, once the signal/background interference becomes available. However, the largest part of the available calculations is not yet equipped with Feynman integrals on the second Riemann sheet (complex poles lie there); furthermore, the largest corrections in the production are from QCD and we could argue that gauge invariance is not an issue over there, so that the OFFP-scheme remains, at the moment, the most pragmatic alternative. Additional considerations with more detailed descriptions are however postponed until Section 4.

Implementation of the CPP-scheme requires some care in the presence of four-leg processes (or more). The natural choice is to perform analytical continuation from real kinematics to complex invariants; consider, for instance, the process $g(p_1) + g(p_2) \rightarrow g(p_3) + \text{H}(p_4)$ where the external H leg is continued from real on-shell mass to s_{H} . For the three invariants,

$$s = -(p_1 + p_2)^2, \quad t = -(p_1 - p_4)^2, \quad u = -(p_1 - p_3)^2, \quad (47)$$

we use the following continuation:

$$t = -\frac{s}{2} \left(1 - \frac{s_{\text{H}}}{s}\right) (1 - \cos \theta), \quad u = -\frac{s}{2} \left(1 - \frac{s_{\text{H}}}{s}\right) (1 + \cos \theta), \quad (48)$$

where θ is the (real) scattering angle (between p_2 and p_3) and $s = 4E^2$, where $2E$ is the (real) energy of center-of-mass system. For the process $g(p_1) + g(p_2) \rightarrow \text{H}(p_3) + \text{H}(p_4)$ where both external H legs are continued from real on-shell mass to s_{H} we obtain

$$t = -\frac{s}{2} \left[1 - \frac{s_{\text{H}}}{s} - \left(1 - 4 \frac{s_{\text{H}}}{s}\right)^{1/2} \cos \theta\right] \quad u = -\frac{s}{2} \left[1 - \frac{s_{\text{H}}}{s} + \left(1 - 4 \frac{s_{\text{H}}}{s}\right)^{1/2} \cos \theta\right]. \quad (49)$$

For a more detailed discussion of the analytic continuation we refer to Appendix C.1. Here we observe that when the problem is with extracting pseudo-observables, e.g. $\Gamma_{\text{H} \rightarrow 4f}$, analytic continuation is performed only after integration over all variables but the Higgs virtuality. The role of pseudo-observables is then very similar to what one had for Lep physics, e.g. the hadronic and leptonic peak cross-sections

$$\sigma_{\text{h}}^0 = 12 \pi \frac{\Gamma_{\text{e}} \Gamma_{\text{h}}}{M_{\text{Z}}^2 \Gamma_{\text{Z}}^2}, \quad \sigma_{\text{l}}^0 = 12 \pi \frac{\Gamma_{\text{e}} \Gamma_{\text{l}}}{M_{\text{Z}}^2 \Gamma_{\text{Z}}^2}, \quad (50)$$

where the POs are fully inclusive. Already at that time it was clear that the expression for realistic observables (RO) at arbitrary s requires a careful examination because of non triviality in off-shell gauge invariance, see Ref. [60].

To summarize, our proposal aims to support the use of Eq.(27) for producing accurate predictions for the Higgs lineshape in the SM; Eq.(27) can be adapted easily for a large class of extensions of the SM. Similarly Eq.(32) should be used to define the Higgs-boson production cross-section instead of σ_{OS} or σ_{OFS} of Eq.(33).

To repeat an obvious argument the zero-width approximation for the Higgs boson is usually reported in comparing experimental studies and theoretical predictions. The approximation has very low quality in the high-mass region where the Higgs boson has a non negligible width. An integration over some distribution is a more accurate estimate of the signal cross-section and we claim that this distribution should be given by the complex propagator and not by some ad hoc Breit–Wigner.

As we have already mentioned most of this paper is devoted to studying the Higgs-boson lineshape in the high-mass region. However, nothing in the formalism is peculiar to that application and the formalism itself forms the basis for extracting pseudo-observables from experimental data. This is a timely contribution to the relevant literature.

3.2 Production cross-section

Before presenting detailed numerical results and comparisons we give the complete definition of the production cross-section; let us define $\zeta = z s$, $\kappa = v s$, and write

$$\sigma^{\text{prod}} = \sum_{i,j} \int \text{PDF} \otimes \sigma_{ij \rightarrow \text{all}}^{\text{prod}} = \sum_{i,j} \int_{z_0}^1 dz \int_z^1 \frac{dv}{v} \mathcal{L}_{ij}(v) \sigma_{ij \rightarrow \text{all}}^{\text{prop}}(\zeta, \kappa, \mu_{\text{R}}, \mu_{\text{F}}), \quad (51)$$

where z_0 is a lower bound on the invariant mass of the H decay products, the luminosity is defined by

$$\mathcal{L}_{ij}(v) = \int_v^1 \frac{dx}{x} f_i(x, \mu_{\text{F}}) f_j\left(\frac{v}{x}, \mu_{\text{F}}\right), \quad (52)$$

where f_i is a parton distribution function and

$$\sigma_{ij \rightarrow \text{all}}^{\text{prop}}(\zeta, \kappa, \mu_{\text{R}}, \mu_{\text{F}}) = \frac{1}{\pi} \sigma_{ij \rightarrow \text{H+X}}(\zeta, \kappa, \mu_{\text{R}}, \mu_{\text{F}}) \frac{\zeta \kappa}{|\zeta - s_{\text{H}}|^2} \frac{\Gamma_{\text{H}}^{\text{tot}}(\zeta)}{\sqrt{\zeta}}. \quad (53)$$

Therefore, $\sigma_{ij \rightarrow \text{H+X}}(\zeta, \kappa, \mu_{\text{R}})$ is the cross section for two partons of invariant mass κ ($z \leq v \leq 1$) to produce a final state containing a H of virtuality $\zeta = z s$ plus jets (X); it is made of several terms (see Ref. [51] for a definition of $\Delta\sigma$),

$$\sum_{ij} \sigma_{ij \rightarrow \text{H+X}}(\zeta, \kappa, \mu_{\text{R}}, \mu_{\text{F}}) = \sigma_{\text{gg} \rightarrow \text{H}} \delta\left(1 - \frac{z}{v}\right) + \frac{s}{\kappa} (\Delta\sigma_{\text{gg} \rightarrow \text{Hg}} + \Delta\sigma_{\text{qg} \rightarrow \text{Hq}} + \Delta\sigma_{\text{q}\bar{\text{q}} \rightarrow \text{Hg}} + \text{NNLO}). \quad (54)$$

As a technical remark the complete phase-space integral for the process $\hat{p}_i + \hat{p}_j \rightarrow p_k + \{f\}$ ($\hat{p}_i = x_i p_i$ etc.) is written as

$$\begin{aligned} \int d\Phi_{ij \rightarrow f} &= \int d\Phi_{\text{prod}} \int d\Phi_{\text{dec}} = \int d^4 p_k \delta^+(p_k^2) \prod_{l=1,n} d^4 q_l \delta^+(q_l^2) \delta^4\left(\hat{p}_i + \hat{p}_j - p_k - \sum_l q_l\right) \\ &= \int d^4 k d^4 Q \delta^+(p_k^2) \delta^4(\hat{p}_i + \hat{p}_j - p_k - Q) \int \prod_{l=1,n} d^4 q_l \delta^+(q_l^2) \delta^4\left(Q - \sum_l q_l\right) \end{aligned} \quad (55)$$

where $\int d\Phi_{\text{dec}}$ is the phase-space for the process $Q \rightarrow \{f\}$ and

$$\begin{aligned} \int d\Phi_{\text{prod}} &= s \int dz \int d^4 p_k d^4 Q \delta^+(p_k^2) \delta(Q^2 - \zeta) \theta(Q_0) \delta^4(\hat{p}_i + \hat{p}_j - p_k - Q) \\ &= s^2 \int dz dv d\hat{t} \int d^4 p_k d^4 Q \delta^+(p_k^2) \delta(Q^2 - \zeta) \theta(Q_0) \delta^4(\hat{p}_i + \hat{p}_j - p_k - Q) \end{aligned}$$

$$\times \delta((\hat{p}_i + \hat{p}_j)^2 - \kappa) \delta((\hat{p}_i + Q)^2 - \hat{t}). \quad (56)$$

Eqs.(51) and (53) follow after folding with PDFs of argument x_i and x_j , after using $x_i = x$, $x_j = v/x$ and after integration over \hat{t} . At NNLO there is an additional parton in the final state and five invariants are need to describe the partonic process, plus the H virtuality. However, one should remember that at NNLO use is made of the effective theory approximation where the Higgs-gluon interaction is described by a local operator. Our variables z, v are related to POWHEG parametrization [55], Y, ξ , by $Y = \ln(x/\sqrt{z})$ and $v = z/(1 - \xi)$.

As already mentioned perturbation theory breaks down in for the complex pole when $\mu_H = 1.74 \text{ TeV}$ (around 930 GeV for on-shell mass). When we consider the lineshape for $\mu_H = 900 \text{ GeV}$ ($\Gamma_{\text{OS}} = 647 \text{ GeV}$) in a window of, at least, $\pm 2\Gamma_{\text{OS}}$ around the peak we go above 2 TeV in the Higgs virtuality; it is worth noting that for $\mu_H = 1.5(2) \text{ TeV}$ the on-shell width is $3.38(15.8) \text{ TeV}$; these results follows from using PROPHECY4F [47] which includes two-loop leading corrections and it is worth observing that the LO result at $\mu_H = 2 \text{ TeV}$ is 3.7 TeV with a 58% one-loop corrections and an estimated 270% two-loop contribution/uncertainty.

These considerations give additional support to the CPP - scheme as the only viable option for defining the Higgs signal in the very high mass region; indeed the $\Gamma_{\text{H}}^{\text{tot}}(s)$ in Eq.(27) is replaced by a $\Gamma_{\text{H}}^{\text{tot}}(s_H)$ in the CPP - scheme. The OFFFP-scheme remains the most pragmatic alternative but the tail of an heavy Higgs boson lineshape extending above $1.3\text{--}1.5 \text{ TeV}$ should be taken with due caution.

4 The issue of gauge invariance

As discussed in Section 2 only the CPP-scheme of Eq.(46) should be used and the background should be included in the calculation. Let us consider the *pragmatic* OFFFP-scheme of Eq.(45) in more detail: here we use the Higgs propagator with its complex pole but production and decay are computed at arbitrary Higgs virtuality and not at the complex pole. As far as LO production is concerned, e.g. the ggH one-loop fermion triangle, there is never an issue of gauge-parameter dependence in going off-shell; in this respect higher order QCD corrections are not a problem.

Consider now the decay, i.e. $\Gamma_{\text{H}}^{\text{tot}}$ in Eq.(32): the amplitude $A(\text{H} \rightarrow \text{F})$, for each final state $|\text{F}\rangle$ and as long as we include the complete set of diagrams at one-loop order, is gauge-parameter independent if the Higgs boson is on its mass-shell. However, as soon as we put an external leg off-shell, the amplitude must be coupled to the corresponding physical source I, i.e. $A(\text{I} \rightarrow \text{H} \rightarrow \text{F})$, and only the complete process $\text{I} \rightarrow \text{F}$ is gauge-parameter independent. The latter does not exclude the existence of subsets of diagrams that satisfy the requirement but this can only be examined case-by-case. To rephrase it, if the Higgs boson is off shell, in LO and NLO QCD in most cases the matrix element still respects gauge invariance, but in NLO EW gauge invariance is lost, unless the CPP-scheme is used.

How to deal with the OFFFP-scheme? Technically speaking, we have a matrix element

$$\Gamma(\text{H} \rightarrow \text{F}) = f(s, \mu_H^2), \quad (57)$$

where s is the virtuality of the external Higgs boson, μ_H is the mass of internal Higgs lines and Higgs wave-function renormalization has been included. The following happens: $f(s_H, s_H)$ is gauge-parameter independent (CPP-scheme) to all orders while $f(\mu_H^2, \mu_H^2)$ is gauge-parameter independent at one-loop but not beyond, $f(s, \mu_H^2)$ is not. In order to account for the off-shellness of the Higgs boson we defined the OFFFP-scheme by choosing (at one loop level) $f(s, s)$, i.e. we intuitively replace the on-shell decay of the Higgs boson of mass μ_H with the *on-shell* decay of an Higgs boson of mass \sqrt{s} and not with the off-shell decay of an Higgs boson of mass μ_H . The same applies for the NLO EW correction to production.

The proof that CPP-scheme satisfies gauge-parameter independence can be sketched as follows:

$$S(s) = \frac{A_{\text{prod}}(s_H) A_{\text{dec}}(s_H)}{[1 + S'_{\text{HH}}(s_H)] (s - s_H)}, \quad \frac{\partial}{\partial \xi} A_{\text{prod,dec}}(s_H) [1 + S'_{\text{HH}}(s_H)]^{-1/2} = 0, \quad (58)$$

where ξ is an arbitrary gauge parameter, $S'_{\text{HH}}(s_{\text{H}})$ is the derivative of $S_{\text{HH}}(s)$ computed at $s = s_{\text{H}}$ and $A_{\text{prod,dec}}$ is the amplitude for production/decay including vertices and wave-function renormalization constants for the external lines. Note that Eq.(58) follows from the use of Nielsen identities, see Ref. [61]. An example is discussed in Appendix A.

At one loop the renormalized Higgs self-energy, computed in the R_ξ -gauge, can be written as

$$S_{\text{HH}}^{(1)}(s, M_{\text{H}}, \xi) = S_{\text{HH}}^{(1)}(s, M_{\text{H}}, \xi = 1) + (s - M_{\text{H}}^2) \Delta S_{\text{HH}}^{(1)}(s, M_{\text{H}}, \xi). \quad (59)$$

Finally, to clarify the statement that $f(\mu_{\text{H}}^2, \mu_{\text{H}}^2)$ may violate gauge invariance beyond one loop we consider the $\text{H} \rightarrow \gamma\gamma$ decay. The LO amplitudes depends on the bare Higgs mass and standard renormalization, introducing the on-shell mass through the real part of the one-loop self-energy, leads to a violation of the Ward-Slavnov-Taylor identities (WSTI), see Refs. [62,63,64]; this will happen at two-loop above the WW threshold. Therefore, the real part of the Higgs self-energy stemming from mass renormalization must be traded for the complex expression, even if the external Higgs boson is assumed to be an on-shell particle.

Eq.(58) gives an additional argument against Breit-Wigner distributions: only the propagator

$$\frac{1}{s - M_{\text{H}}^2 + S_{\text{HH}}(s)} = Z_{\text{HH}}^{-1/2} \frac{1}{s - s_{\text{H}}} Z_{\text{HH}}^{-1/2}, \quad Z_{\text{HH}} = 1 + \frac{S_{\text{HH}}(s) - S_{\text{HH}}(s_{\text{H}})}{s - s_{\text{H}}}, \quad (60)$$

reproduces the correct factors to be combined with production and decay vertices.

To conclude the discussion we summarize few well-known points which, however, are not always taken into proper account. Consider the partial decay width $\text{H} \rightarrow \text{WW}$, hiding the fact that also the Ws are unstable objects; one way of constructing it is to consider the amplitude for the process and derive at tree-level the following expression:

$$\begin{aligned} \Gamma_{\text{H} \rightarrow \text{WW}}^{\text{OS}} &= \frac{1}{M_{\text{H}}} \int d\Phi_{\text{H} \rightarrow \text{WW}} \left| A_{\text{H} \rightarrow \text{WW}} \right|^2 \\ &= \frac{G_{\text{F}} M_{\text{H}}^3}{8\sqrt{2}\pi} \left(1 - 4 \frac{M_{\text{W}}^2}{M_{\text{H}}^2} + 12 \frac{M_{\text{W}}^4}{M_{\text{H}}^4} \right) \beta_{\text{W}}(M_{\text{H}}^2), \quad \beta_{\text{W}}^2(M_{\text{H}}^2) = 1 - 4 \frac{M_{\text{W}}^2}{M_{\text{H}}^2}. \end{aligned} \quad (61)$$

Next we compute the imaginary part of the one-loop H self-energy due to internal charged lines. We obtain:

$$\begin{aligned} \text{Im } S_{\text{HH}}^{\text{ch}}(s) &= s^{1/2} \Gamma_{\text{H}}^{\text{ch,inv}}(s) \theta(s - 4 M_{\text{W}}^2) + \Delta_{\text{H}}^{\text{ch}}(s) \theta(s - 4 \xi M_{\text{W}}^2), \\ \Gamma_{\text{H}}^{\text{ch,inv}}(s) &= \frac{G_{\text{F}} s^{3/2}}{8\sqrt{2}\pi} \left(1 - 4 \frac{M_{\text{W}}^2}{s} + 12 \frac{M_{\text{W}}^4}{s^2} \right) \beta_{\text{W}}(s), \\ \Delta_{\text{H}}^{\text{ch}}(s) &= - \frac{G_{\text{F}} s^2}{8\sqrt{2}\pi} \left(1 - \frac{M_{\text{H}}^4}{s^2} \right) \left(1 - 4 \xi \frac{M_{\text{W}}^2}{s} \right)^{1/2}. \end{aligned} \quad (62)$$

Unitarity of the theory requires proportionality between $\Gamma_{\text{H} \rightarrow \text{WW}}^{\text{OS}}$ and $\text{Im } S_{\text{HH}}^{\text{ch}}$. This is never a problem for the fermion final states but we see already the paradox in the bosonic sector: from one side we compute $\text{H} \rightarrow \text{WW}$, from the other all charged bosonic lines (physical or not) circulate in the loop. It is trivially true that

$$\Gamma_{\text{H} \rightarrow \text{WW}}^{\text{OS}} = \Gamma_{\text{H}}^{\text{ch,inv}}(M_{\text{H}}^2) = \frac{1}{M_{\text{H}}} \text{Im } S_{\text{HH}}^{\text{ch}}(M_{\text{H}}^2), \quad (63)$$

a result that satisfies unitarity and gauge invariance; however, going off-shell is different. There are matters of principle that do not matter in practice: if we consider a ‘light’ Higgs, say below 200 GeV, the difference between the on-shell width computed in the R_ξ -gauge and γ_{H} is tiny and, aside from the neighborhoods of unphysical thresholds ($\xi = M_{\text{H}}^2/(4M_{\text{W}}^2)$, $\xi = M_{\text{H}}^2/(4M_{\text{Z}}^2)$), negligible over a wide range of values of the gauge parameter ξ [31]. However, consider a typical implementation of the H production cross-section:

$$\int ds \frac{s^{1/2} \Gamma_{\text{H}}(s)}{\pi} \frac{\sigma_{ij \rightarrow \text{H}}(s)}{(s - M_{\text{H}}^2)^2 + M_{\text{H}}^2 \Gamma_{\text{H}}(M_{\text{H}}^2)}. \quad (64)$$

What it is meant by $\Gamma_{\text{H}}(M_{\text{H}}^2)$ in the denominator of Eq.(64)? Since we are dealing with the denominator of the propagation function for a Higgs boson of virtuality s and since we would like to respect unitarity, it has to be interpreted as the imaginary part of the self-energy. At one loop, for $s = M_{\text{H}}^2$ gauge invariance is not violated. But what about the $\Gamma_{\text{H}}(s)$ that appears in the numerator? Again, because of unitarity, it should be interpreted as the imaginary part of the off-shell self-energy, i.e. the self-energy for a H of mass M_{H} and virtuality s ; however, this quantity has a ξ -dependent part which is a function of the Higgs virtuality. Therefore, no matter how small is the on-shell width for a light Higgs boson, there will be an s and ξ -dependent distortion of the lineshape. Of course there will never be a problem for a calculation assembling the whole process in one stroke; however, defining the signal is another story.

We conclude this Section by showing explicitly the delicate point in extracting the pseudo-observable *decay width* from the complete amplitude. We have

$$\begin{aligned}
S(s) &= \left[1 + \frac{S_{\text{HH}}(s) - S_{\text{HH}}(s_{\text{H}})}{s - s_{\text{H}}}\right]^{-1} A_{\text{prod}}(s) \frac{1}{s - s_{\text{H}}} A_{\text{dec}}(s) \\
&= A_{\text{prod}}(s) \left[1 + \frac{S_{\text{HH}}(s) - S_{\text{HH}}(s_{\text{H}})}{s - s_{\text{H}}}\right]^{-1/2} \frac{1}{s - s_{\text{H}}} \left[1 + \frac{S_{\text{HH}}(s) - S_{\text{HH}}(s_{\text{H}})}{s - s_{\text{H}}}\right]^{-1/2} \\
&\quad \times \left\{ A_{\text{dec}}(s_{\text{H}}) + \left[A_{\text{dec}}(s) - A_{\text{dec}}(s_{\text{H}}) \right] \right\} \\
&= S_{\text{prod}}(s) \frac{1}{s - s_{\text{H}}} S_{\text{dec}}(s),
\end{aligned} \tag{65}$$

where the matrix element for the *decay* can be decomposed into

$$\begin{aligned}
S_{\text{dec}}(s) &= \left[1 + \frac{1}{2} X_{\text{HH}}(s)\right] Z_{\text{H}}^{-1/2} A_{\text{dec}}(s_{\text{H}}) + \left[1 - \frac{1}{2} Y_{\text{HH}}(s)\right] \left[A_{\text{dec}}(s) - A_{\text{dec}}(s_{\text{H}}) \right], \\
X_{\text{HH}}(s) &= S'_{\text{HH}}(s_{\text{H}}) - \frac{S_{\text{HH}}(s) - S_{\text{HH}}(s_{\text{H}})}{s - s_{\text{H}}}, \quad Y_{\text{HH}}(s) = \frac{S_{\text{HH}}(s) - S_{\text{HH}}(s_{\text{H}})}{s - s_{\text{H}}}.
\end{aligned} \tag{66}$$

The decay width is defined in terms of $Z_{\text{H}}^{-1/2} A_{\text{dec}}(s_{\text{H}})$ while the rest is $\mathcal{O}(s - s_{\text{H}})$.

5 Numerical results

In the following we will present numerical results obtained with the program HTO (G. Passarino, unpublished) that allows for the study of the Higgs–boson-lineshape, in gluon-gluon fusion (ggF), using complex poles. HTO is a FORTRAN 95 program that contains a translation of the subroutine HIGGSNNLO written by M. Grazzini for computing the total (on-shell) cross-section for Higgs-boson production (in ggF) at NLO and NNLO [65,66,67] (HTO has a library for one-loop integrals that extends the one of Ref. [68]). It is worth noting that the ggF production mechanism dominates up to $\mu_{\text{H}} = 700 \text{ GeV}$ but for higher masses the vector-boson fusion (VBF) mechanism starts to compete, with a ratio ggF/VBF of 1.11 at 1 *TeV*. The following acronyms will be used:

FW Breit–Wigner Fixed Width (Eq.(35))

RW Breit–Wigner Running Width (Eq.(34))

OS parameters in the On-Shell scheme

Bar parameters in Bar-scheme (Eq.(36))

FS QCD renormalization (factorization) scales fixed

RS QCD renormalization (factorization) scales running

Table 3: The re-weighting factor w for the (total) integrated Higgs lineshape, $\sigma^{\text{prop}}/\sigma^{\text{BW}}$ using $\gamma_{\text{H}} = \Gamma_{\text{H}}^{\text{OS}}$ in Eq.(32).

μ_{H} [GeV]	$\Gamma_{\text{H}}^{\text{OS}}$ [GeV]	σ^{OS} [pb]	σ^{BW} [pb]	σ^{prop} [pb]	w
200	1.43	5.249	5.674	5.459	0.962
300	8.43	2.418	2.724	2.585	0.949
400	29.2	2.035	1.998	1.927	0.964
500	68.0	0.8497	0.8108	0.7827	0.965
600	123.0	0.3275	0.3231	0.3073	0.951

All results in this paper (but those in Table 13) refer to $\sqrt{s} = 7 \text{ TeV}$ and are based on the MSTW2008 PDF sets [69]. For complex W, Z poles we use Eq.(9) with HXSWG standard input. For the t complex pole we use [70]

$$\sqrt{s_{\text{t}}} = M_{\text{t}}^{\text{OS}} - \frac{i}{2} \Gamma_{\text{t}}^{\text{OS}}, \quad (67)$$

with a LO on-shell width

$$\Gamma_{\text{t}}^{\text{OS}} = \frac{G_{\text{F}}}{8\sqrt{2}\pi} \left(M_{\text{t}}^2 - M_{\text{W}}^2 \right)^2 \frac{M_{\text{t}}^2 + 2 M_{\text{W}}^2}{M_{\text{t}}^3}, \quad (68)$$

with an on-shell mass $M_{\text{t}} = M_{\text{t}}^{\text{OS}} = 172.5 \text{ GeV}$.

The integrand in Eq.(51) has several peaks; the most evident is in the propagator and in HTO a change of variable is performed,

$$\zeta = \frac{1}{1 + (\mu_{\text{H}}/\gamma_{\text{H}})^2} \left[\mu_{\text{H}}^2 + \mu_{\text{H}} \gamma_{\text{H}} \tan(\mu_{\text{H}} \gamma_{\text{H}} z') \right],$$

$$z' = \frac{s}{\mu_{\text{H}} \gamma_{\text{H}}} \left[(a_{\text{m}} + a_{\text{M}}) \zeta - a_{\text{m}} \right], \quad a_{\text{m}} = \arctan \frac{\mu_{\text{H}}^2 - z_0 s}{\mu_{\text{H}} \gamma_{\text{H}}}, \quad a_{\text{M}} = \arctan \frac{s - \mu_{\text{H}}^2}{\mu_{\text{H}} \gamma_{\text{H}}}. \quad (69)$$

Similarly, another change is performed

$$v = \exp\{(1 - u^2) \ln z\}, \quad x = \exp\{(1 - y^2) \ln v\}. \quad (70)$$

In comparing the OFFBW-scheme with the OFFP-scheme one should realize that there are two sources of difference, the functional form of the distributions and the different numerical values of the parameters in the distributions. To understand the impact of the functional form we have performed a comparison where (unrealistically) $\gamma_{\text{H}} = \Gamma_{\text{H}}^{\text{OS}}$ is used in the Higgs propagator; results are shown in Table 3.

In Table 4 we compare the on-shell production cross-section as given in Ref. [1] with the off-shell cross-section in the OFFBW-scheme (Eq.(43)) and in the OFFP-scheme (Eq.(45)). The total Higgs boson width, present in Eq.(28), is computed by interpolating the tables of Ref. [1].

An important question regarding the numerical impact of a calculation where the on-shell Higgs boson is left off-shell and convoluted with some distribution is how much of the effect survives the inclusion of theoretical uncertainties. In the OFFBW-scheme we can compare with the results of Ref. [21], at least for values of the Higgs boson mass where their results are available, i.e. below 300 GeV. We compare with Tables 2–3 of Ref. [1] at 300 GeV and obtain the results shown in Table 5 where only the QCD scale uncertainty is included. At these values of the Higgs boson mass both on-shell production and off-shell production, sampled over a Breit–Wigner, are compatible within the errors. The OFFP-scheme gives a slightly higher central value of 2.86 pb. The comparison shows drastically different results for high values of the mass where the difference in central values is much bigger than the theoretical uncertainty.

In Table 6 we show a more detailed comparison of the production cross-section in the OFFBW-scheme between iHIXS of Ref. [21] and our calculation. Δ is the percentage error due to QCD scales and δ is the percentage ratio HTO/iHIXS.

Table 4: Comparison of the on-shell production cross-section as given in Ref. [1] with the off-shell cross-section in the OFFBW-scheme (Eq.(43)) and in the OFFP-scheme (Eq.(45)).

μ_H [GeV]	Γ_H^{OS} [GeV]	γ_H [GeV]	σ^{OS} [pb]	σ^{BW} [pb]	σ^{prop} [pb]
500	68.0	60.2	0.8497	0.8239	0.9367
550	93.1	82.8	0.5259	0.5161	0.5912
600	123	109	0.3275	0.3287	0.3784
650	158	139	0.2064	0.2154	0.2482
700	199	174	0.1320	0.1456	0.1677
750	248	205	0.0859	0.1013	0.1171
800	304	245	0.0567	0.0733	0.0850
850	371	277	0.0379	0.0545	0.0643
900	449	331	0.0256	0.0417	0.0509

Table 5: The production cross-section in pb at $\mu_H = 300 \text{ GeV}$. Result from HTO is computed with running QCD scales.

Tab. 2 of Ref. [1]	Tab. 3 of Ref. [1]	Tab. 5 of Ref. [21]	HTO RS-option
$2.42^{+0.14}_{-0.15}$	$2.45^{+0.16}_{-0.22}$	$2.57^{+0.15}_{-0.22}$	$2.81^{+0.25}_{-0.23}$

Table 6: Comparison of the production cross-section in the OFFBW-scheme between iHIXS (Table 5 of Ref. [21]) and our calculation. Δ is the percentage error due to QCD scales and δ is the percentage ratio HTO/iHIXS.

μ_H [GeV]	σ_{iHIXS} [pb]	Δ_{iHIXS} [%]	σ_{HTO} [pb]	Δ_{HTO} [%]	δ [%]
200	5.57	+7.19 -9.06	5.63	+9.12 -9.30	1.08
220	4.54	+6.92 -8.99	4.63	+8.93 -8.85	1.98
240	3.80	+6.68 -8.91	3.91	+8.76 -8.51	2.89
260	3.25	+6.44 -8.84	3.37	+8.61 -8.22	3.69
280	2.85	+6.18 -8.74	2.97	+8.49 -7.98	4.21
300	2.57	+5.89 -8.58	2.69	+8.36 -7.75	4.67

Table 7: Scaling factor OFFP/OFFBW schemes (Eqs.(45) and (43)) for the invariant mass windows of Eq.(72).

$\mu_{\text{H}}[\text{GeV}]$	$n = -4$	$n = -3$	$n = -2$	$n = -1$	$n = 0$	$n = 1$	$n = 2$	$n = 3$
500	1.24	1.13	1.08	1.23	1.32	1.11	0.97	0.88
600	1.39	1.20	1.08	1.27	1.40	1.12	0.94	0.84
650	1.50	1.24	1.08	1.30	1.44	1.13	0.93	0.81
700	1.62	1.28	1.09	1.34	1.49	1.13	0.92	0.79
750	1.78	1.34	1.10	1.41	1.57	1.14	0.90	0.77
800	1.99	1.41	1.12	1.49	1.64	1.14	0.89	0.75

Another quantity that is useful in describing the lineshape is obtained by introducing the peak mass,

$$M_{\text{peak}}^2 = (M_{\text{H}}^{\text{OS}})^2 + (\Gamma_{\text{H}}^{\text{OS}})^2, \quad (71)$$

an by considering the following windows in the invariant mass,

$$\left[M_{\text{peak}} + \frac{n}{2} \Gamma_{\text{H}}^{\text{OS}}, M_{\text{peak}} + \frac{n+1}{2} \Gamma_{\text{H}}^{\text{OS}} \right], \quad n = 0, \pm 1, \dots \quad (72)$$

In Table 7 we present the ratio OFFP/OFFBW for the invariant mass distribution in the windows of Eq.(72).

In Table 8 we include uncertainties in the comparison; both OFFBW and OFFP are computed with the RS option, i.e. running QCD scales instead of a fixed one. Note that for $\sigma(\mu)$ we define a central value $\sigma_c = \sigma(\bar{\mu})$ and a scale error as $[\sigma^-, \sigma^+]$ where

$$\sigma^- = \min_{\mu \in [\bar{\mu}/2, 2\bar{\mu}]} \sigma(\mu), \quad \sigma^+ = \max_{\mu \in [\bar{\mu}/2, 2\bar{\mu}]} \sigma(\mu), \quad (73)$$

and where $\mu = \mu_{\text{R}} = \mu_{\text{F}}$ and $\bar{\mu}$ is the reference scale, static or dynamic.

In Table 9 we compare results from Table 5 of Ref. [21] with our OFFBW results with two options: 1) $\mu_{\text{R}}^2, \mu_{\text{F}}^2$ are fixed, 2) they run with $\zeta/4$. For three values of μ_{H} reported we find differences of 2.0%, 3.7% and 4.7%, compatible with the scale uncertainty. Furthermore, we use Ref. [1] for input parameters which differ slightly from the one used in Ref. [21]. Note that also the functional form of the Breit–Wigner is different since their default value is not the one in Eq.(34) but

$$\text{BW}(s) = \frac{1}{\pi} \frac{\sqrt{s} \Gamma_{\text{H}}(\sqrt{s})}{\left(s - \mu_{\text{H}}^2 \right)^2 + \mu_{\text{H}}^2 \Gamma_{\text{H}}^2(\mu_{\text{H}})}, \quad (74)$$

where $\Gamma_{\text{H}}(\sqrt{s})$ is the decay width of a Higgs boson at rest with mass \sqrt{s} .

In Table 10 we use the OFFP-scheme of Eq.(45) and look for the effect of running QCD scales in the H invariant mass distribution. Differences are of the order of 2–3% apart from the high-mass side of the distribution for very high H masses. As we have mentioned already, the only scheme respecting gauge invariance that allows us for a proper definition of pseudo-observables is the CPP-scheme of Eq.(46). It requires analytical continuation of the Feynman integrals into the second Riemann sheet. Once again, the definition of POs is conventional but should put in one-to-one correspondence well-defined theoretical predictions with derived experimental data.

In Table 11 we give a simple example by considering the process $gg \rightarrow \text{H}$ at lowest order and compare the traditional on-shell production cross-section, see the l.h.s. of Eq.(33), with the production cross-section as defined in the CPP-scheme. Therefore we only consider $gg \rightarrow H$ at LO (i.e. $v = z$) and put H on its real mass-shell or on the complex one. Below 300 GeV there is no visible difference, at 300 GeV the two results start to differ with an increasing gap up to 600 GeV after which there is a plateau of about 25% for higher values of μ_{H} .

Table 8: Production cross section with errors due to QCD scale variation and PDF uncertainty. First entry is the on-shell cross-section of Table 2 of Ref. [1], second entry is OFFBW (Eq.(43)), last entry is OFFP Eq.(45).

μ_H [GeV]	σ [pb]	Scale [%]	PDF [%]
600	0.336	+ 6.1 - 5.2	+ 6.2 - 5.3
	0.329	+ 11.2 - 11.3	+ 4.7 - 4.8
	0.378	+ 9.7 - 10.0	+ 5.0 - 3.9
650	0.212	+ 6.2 - 5.2	+ 6.5 - 5.5
	0.215	+ 12.4 - 12.2	+ 5.1 - 5.3
	0.248	+ 10.2 - 10.0	+ 5.3 - 4.2
700	0.136	+ 6.3 - 5.3	+ 6.9 - 5.8
	0.146	+ 13.9 - 13.3	+ 5.6 - 5.8
	0.168	+ 11.0 - 11.1	+ 5.5 - 4.6
750	0.0889	+ 6.4 - 5.4	+ 7.2 - 6.1
	0.101	+ 15.8 - 14.5	+ 6.1 - 6.3
	0.117	+ 12.2 - 11.9	+ 5.8 - 5.1
800	0.0588	+ 6.5 - 5.4	+ 7.6 - 6.3
	0.0733	+ 18.0 - 16.0	+ 6.7 - 6.9
	0.0850	+ 13.7 - 13.0	+ 6.1 - 5.5
850	0.0394	+ 6.5 - 5.5	+ 8.0 - 6.6
	0.0545	+ 20.4 - 17.6	+ 7.2 - 7.5
	0.0643	+ 15.7 - 14.3	+ 6.5 - 6.0
900	0.0267	+ 6.7 - 5.6	+ 8.3 - 6.9
	0.0417	+ 22.8 - 19.1	+ 7.7 - 8.0
	0.0509	+ 18.1 - 16.0	+ 7.0 - 6.6

Table 9: Comparison of results from Table 5 of Ref. [21] with our OFFBW results (Eq.(43)) with two options: 1) μ_R^2, μ_F^2 are fixed, 2) they run with $\zeta/4$.

μ_H [GeV]	iHIXS		HTO			
	σ [pb]	Scale [%]	σ_1 [pb]	Scale [%]	σ_2 [pb]	Scale [%]
220	4.54	+ 6.9 - 9.0	4.63	+ 8.9 - 8.9	4.74	+ 7.3 - 8.7
260	3.25	+ 6.4 - 8.8	3.37	+ 8.6 - 8.2	3.49	+ 7.9 - 8.6
300	2.57	+ 5.9 - 8.6	2.69	+ 8.4 - 7.8	2.81	+ 8.4 - 8.5

Table 10: Scaling factor in the OFFP-scheme (Eq.(45)) running/fixed QCD scales for the invariant mass distribution. Here $[x, y] = [M_{\text{peak}} + x \Gamma_H^{\text{OS}}, M_{\text{peak}} + y \Gamma_H^{\text{OS}}]$.

μ_H [GeV]	$[-1, -\frac{1}{2}]$	$[-\frac{1}{2}, -\frac{1}{4}]$	$[-\frac{1}{4}, 0]$	$[0, \frac{1}{4}]$	$[\frac{1}{4}, \frac{1}{2}]$	$[\frac{1}{2}, 1]$
600	1.023	1.021	1.019	1.018	1.017	1.016
700	1.027	1.023	1.021	1.019	1.018	1.019
800	1.030	1.024	1.021	1.021	1.021	1.136

Table 11: γ_H and Γ_H^{OS} as a function of μ_H . We also report the ratio between the LO cross-sections for $gg \rightarrow H$ in the CPP-scheme and in the OS-scheme.

μ_H [GeV]	γ_H [GeV]	Γ_H^{OS} [GeV]	$\sigma_{\text{CPP}}(s_H) / \sigma_{\text{OS}}(M_H^{\text{OS}})$
300	7.58	8.43	0.999
350	14.93	15.20	1.086
400	26.66	29.20	1.155
450	41.18	46.90	1.183
500	58.85	68.00	1.204
550	79.80	93.10	1.221
600	104.16	123.00	1.236
650	131.98	158.00	1.248
700	163.26	199.00	1.256
750	197.96	248.00	1.262
800	235.93	304.00	1.264
850	277.00	371.00	1.263
900	320.96	449.00	1.258
950	367.57	540.00	1.252
1000	416.57	647.00	1.242

The production cross-section in Eq.(54) is made of one term corresponding to $gg \rightarrow H$ which we denote by σ^0 and terms with at least one additional jet, σ^j . The invariant mass of the two partons in the initial state is $\kappa = v s$ with $z \leq v \leq 1$, ζ being the Higgs virtuality. In Table 12 we introduce a cut such that

$$z \leq v \leq \min\{v_c z, 1\} \quad (75)$$

and study the dependence of the result on v_c by considering $\sigma^t = \sigma^0 + \sigma^j$ and $\delta = \sigma_c^t / \sigma^t$. The results show that a cut $z \leq v \leq 1.01 z$ gives already 85% of the total answer.

LHC is now running with a center of mass energy of 8 *TeV*; in Table 13 we have shown a comparison for the production cross-section at 7 *TeV* and 8 *TeV*.

On the left-hand side of Figure 1 we compare the production cross-section as computed with the OFFP-scheme of Eq.(45) or with the OFFBW-scheme of Eq.(43) for $\mu_H = 600$ *GeV*. For the OFFBW-scheme we use Breit–Wigner parameters in the OS-scheme (red curve) and in the Bar-scheme of Eq.(36) (blue curve). Deviations from the OFFP-scheme are maximal in the OS-scheme and much less pronounced in the Bar-scheme.

On the right-hand side of Figure 1 we show the effect of using dynamical QCD scales (invariant mass of the di-photon system) for the $gg \rightarrow H + X \rightarrow X + \gamma\gamma$ cross-section at $\mu_H = 400$ *GeV*.

On the left-hand side of Figure 2 we consider the on-shell production cross-section $\sigma^{\text{OS}}(\text{pp} \rightarrow H)$ (black curve) which includes convolution with PDFs. The blue curve gives the off-shell production cross-section sampled over the (complex) Higgs propagator while the red curves is sampled over a Breit–Wigner distribution. The observed effect is substantial even in the low mass region.

On the right-hand side of Figure 2 we show differential *K* factors ($\sigma_{\text{NLO}}/\sigma_{\text{LO}}$ etc.) for the process $\text{pp} \rightarrow (H \rightarrow 4e) + X$, comparing the fixed QCD scale option, $\mu_R = \mu_F = M_H/2$, and the running scale option, $\mu_R = \mu_F = M(4e)/2$. For running QCD scales the *K* factor is practically constant over a wide range of the Higgs virtuality.

On the left-hand side of Figure 3 we show the normalized invariant mass distribution in the OFFP-scheme with running QCD scales for Higgs-boson masses of 600 *GeV* (black), 700 *GeV* (blue), 800 *GeV* (red) in the windows $M_{\text{peak}} \pm 2\Gamma_{\text{OS}}$ where M_{peak} is defined in Eq.(71).

On the right-hand side of Figure 3 we show the normalized invariant mass distribution in the OFFP-scheme (blue) and OFFBW-scheme (red) with running QCD scales for a Higgs-boson mass of 800 *GeV* in the window $M_{\text{peak}} \pm 2\Gamma_{\text{OS}}$.

Table 12: The effect of introducing a cut on the invariant mass of the initial-state partons.

μ_H [GeV]	v_c	σ^0 [pb]	σ^J [pb]	σ^t [pb]	δ [%]
600	no cut	0.2677	0.1107	0.3784	
	1.001		0.0127	0.2804	74
	1.01		0.0473	0.3149	83
	1.05		0.0918	0.3595	95
700	no cut	0.1208	0.0469	0.1677	
	1.001		0.0054	0.1262	75
	1.01		0.0201	0.1409	84
	1.05		0.0391	0.1599	95
800	no cut	0.0632	0.0218	0.0850	
	1.001		0.0025	0.0657	77
	1.01		0.0094	0.0726	85
	1.05		0.0182	0.0814	96

Table 13: Comparison of the production cross-sections in the OFFP-scheme (Eq.(45)) at 7 TeV and 8 TeV.

μ_H [GeV]	σ [pb] 7 TeV	σ [pb] 8 TeV	ratio
600	0.378	0.587	1.55
650	0.248	0.392	1.58
700	0.168	0.271	1.67
750	0.117	0.194	1.67
800	0.0850	0.145	1.77
850	0.0643	0.113	1.77
900	0.0509	0.0922	1.87

Finally, in Figure 4 we show the normalized invariant mass distribution in the OFFP-scheme with running QCD scales at 600–800 GeV in the window $M_{\text{peak}} \pm 2\Gamma_{\text{OS}}$ for 7 TeV (blue) and 8 TeV (red). The invariant mass distribution in the OFFP-scheme with running QCD scales for a Higgs-boson mass of 800 GeV (in the window $M_{\text{peak}} \pm 2\Gamma_{\text{OS}}$) is shown in Figure 5; the blue line refers to a center-of-mass energy of 8 TeV, the red one to 7 TeV.

5.1 Results in CPP-scheme

Here, we will briefly summarize what was covered in Section 3.1 for the CPP-scheme. referring to Eq.(53) we can say the following: the production amplitude, including QCD corrections, is always ξ -independent and we can keep full off-shellness; the decay amplitude, beyond LO, is not and should be evaluated at the Higgs complex pole in the CPP-scheme. To give an example of the results we select the process $gg \rightarrow H \rightarrow Z^c Z^c$, where the two Z-bosons in the final state are also taken at their complex pole, thus giving a full gauge-invariant quantity. We will show results in the OFFP-scheme (Eq.(45)) and in the CPP-scheme (Eq.(46)). Caveat emptor: one should not interpret their difference as a source of theoretical uncertainty since comparisons should only take place for the full $S \oplus B$ matrix element and what we are doing in the two schemes simply amounts to shifting some part from the known S-amplitude to the unknown S/B-interference. Furthermore, only the CPP-scheme is a fully consistent recipe to *define* a gauge-invariant signal; the only reason why we presented most of our results in the OFFP-scheme is that it is much simpler to implement in any preexisting calculation while the CPP-scheme requires analytical continuation into the second Riemann sheet.

In Figure 8 we show the invariant mass distribution in the OFFP-scheme (black) and in the CPP-scheme (red) for $\mu_H = 700$ GeV (left) and $\mu_H = 800$ GeV (right) in the window $[M_{\text{peak}} - M_{\text{peak}} + 2\Gamma_{\text{OS}}]$ for the

Table 14: Comparison of the production cross-sections at 8 TeV : OFFBW-scheme, OFFP-scheme, on-shell results of Ref. [71] and the Breit-Wigner approach of Ref. [22].

$\mu_H[\text{GeV}]$	$\sigma[\text{pb}]$ OFFBW	$\sigma[\text{pb}]$ OFFP	$\sigma[\text{pb}]$ Ref. [71]	$\sigma[\text{pb}]$ Ref. [22]
300	3.74	3.87	3.32	3.45
280	4.10	4.25	3.67	3.82
260	4.60	4.79	4.16	4.34
240	5.29	5.53	4.82	5.05
220	6.21	6.43	5.71	6.00
200	7.48	7.53	6.95	7.32
190	8.31	8.35	7.78	8.21
180	9.42	9.45	8.85	9.42
170	10.59	10.62	10.11	10.72
160	12.24	12.24	11.76	12.66
150	13.88	13.88	13.57	14.43
140	15.78	15.79	15.59	16.53
130	18.05	18.05	18.04	19.14
125	19.41	19.41	19.49	20.69

process $gg \rightarrow H \rightarrow Z^c Z^c$. The shoulder in the low mass side of the resonance (in the CPP-scheme) is due to the fact that the H-width is very large, the production cross-section is increasing for decreasing invariant mass and there is no suppression from the decay which is taken at the Higgs complex pole. Thus, the decrease in the distribution for small invariant masses is delayed by the large width. The high invariant mass behavior reflects again a constant (at the complex pole) decay amplitude.

5.2 Results in the low Higgs mass region

For lower values of the Higgs mass we compare the OFFBW-scheme and the OFFP one (based on Eq.(17)) at 8 TeV in Table 14; here we also show the on-shell results of Ref. [71] and the Breit-Wigner (running width scheme) approach of Ref. [22]. The results of Table 14 show a good convergence of OFFBW/OFFP results to the on-shell ones for low values of the Higgs mass.

6 QCD scale error

The conventional theoretical uncertainty associated with QCD scale variation is defined in Eq.(73). Let us consider the production cross-section at 800 GeV in the OFFP-scheme with running or fixed QCD scales, we obtain

$$\text{RS } 0.08497^{+13.7\%}_{-13.0\%}, \quad \text{FS } 0.07185^{+6.7\%}_{-8.5\%}. \quad (76)$$

The uncertainty with running scales is about twice the one where the scales are kept fixed. One might wonder which is the major source and we have done the following; in estimating the conventional uncertainty in the RS-option we keep $\mu_F^2 = \bar{\mu}^2 = \zeta/4$ and vary μ_R between $\bar{\mu}/2$ and $2\bar{\mu}$. The corresponding result is

$$\text{RS } 0.08497^{+3.9\%}_{-4.4\%}, \quad \mu_R \text{ only}. \quad (77)$$

Therefore, the main source of uncertainty comes from varying the factorization scale. However, in the fixed-scale option we obtain

$$\text{FS } 0.07185^{+3.6\%}_{-4.4\%}, \quad \mu_R \text{ only} \quad (78)$$

and μ_F -variation is less dominant. In any case the question of which variation is dominating depends on the mass-range; indeed, in the ONBW-scheme with fixed scales at 140 GeV we have

$$\text{ONBW } 12.27^{+11.1\%}_{-10.1\%}, \quad \mu_R \text{ and } \mu_F$$

$$\text{ONBW} \quad 12.27 \begin{matrix} +8.7\% \\ -9.6\% \end{matrix}, \quad \mu_R \quad \text{only} \quad (79)$$

showing μ_R dominance.

In order to compare this conventional definition of uncertainty with the work of Ref. [72] we recall their definition of $p\%$ credible interval; given a series

$$\sigma = \sum_{n=l}^k c_n \alpha_s^n, \quad (80)$$

the $p\%$ credible interval $\sigma \pm \Delta\sigma^p$ is defined as

$$\begin{aligned} \Delta\sigma^p &= \alpha_s^{k+1} \max(\{c\}) \frac{n_c + 1}{n_c} p\%, & p\% \leq \frac{n_c}{n_c + 1}, \\ \Delta\sigma^p &= \alpha_s^{k+1} \max(\{c\}) \left[(n_c + 1) (1 - p\%) \right]^{-1/n_c}, & p\% \geq \frac{n_c}{n_c + 1}, \end{aligned} \quad (81)$$

with $n_c = k - l + 1$. Using this definition we find that the 68%(90%) credible interval for μ_R uncertainty in the production cross-section at 800 GeV is 3.1%(5.3%) in substantial agreement with the conventional method. For ONBW-scheme at 140 GeV the 90% credible interval for μ_R uncertainty is 8.0%. It could be interesting to extend the method of Ref. [72] to cover μ_F uncertainty.

7 Residual theoretical uncertainty

As we mentioned before the accuracy at which the imaginary part of s_H can be computed is not of the same quality as the next-to-leading-order (NLO) accuracy of the on-shell width. It would be desirable to include two- and three-loop contributions as well in γ_H and for some of these contributions only on-shell results have been computed so far. Here we follow the analysis of Ref. [18] where the authors try to improve the solution of the complex pole equation by using the available on-shell information. It is again a method based on some expansion and does not include the full SM, QCD corrections and complex poles for internal W, Z lines; it amounts to consider only the Higgs-Goldstone Lagrangian of the SM. Nevertheless it is very useful to give a rough estimate of the missing orders. The authors of Ref. [18] define a double expansion of the self-energy,

$$S_{HH}(s) = A M_H^2 + B(s - M_H^2) + \frac{C}{M_H^2} (s - M_H^2)^2 + \dots \quad A = \sum_{n=0}^{\infty} a_n \left(\frac{G_F M_H^2}{2\sqrt{2}\pi^2} \right)^n, \quad (82)$$

etc. In this way we can write

$$\gamma_H = \frac{G_F M_H^3}{2\sqrt{2}\pi^2} a_1 \left(1 + \frac{G_F M_H^2}{2\sqrt{2}\pi^2} \frac{a_2}{a_1} + \dots \right). \quad (83)$$

The ratio a_2/a_1 has been computed and we can estimate that the first correction to γ_H is roughly given by

$$\delta_H = 0.350119 \frac{G_F \mu_H^2}{2\sqrt{2}\pi^2}. \quad (84)$$

Changes in γ_H range from 2.3% at 400 GeV to 9.4% at 750 GeV. In general, from Ref. [18] we do not see very large variations up to 1TeV with a breakdown of the perturbative expansion around when 1.74 TeV. Let us elaborate a bit more: in the Higgs-Goldstone model one has

$$\frac{\gamma_H}{\mu_H} = 1.1781 g_H + 0.4125 g_H^2 + 1.1445 g_H^3 \quad g_H = \frac{G_F \mu_H^2}{2\sqrt{2}\pi^2}, \quad (85)$$

Table 15: Theoretical uncertainty on the production cross-section, the height of the maximum, the position of the half-maxima and the area of the resonance.

$\mu_{\text{H}}[\text{GeV}]$	$\delta_{\text{H}}[\%]$	$\delta\sigma^{\text{prod}}[\%]$	$\delta\Sigma_{\text{max}}[\%]$	$\Delta\zeta_{-}, \Delta\zeta_{+}[\text{GeV}]$	$\delta A[\%]$
600	5.3	-6.0 +6.3	-10.8 +11.4	(-2.5, +2.5) (+2.5, -2.5)	-4.8 +6.0
700	7.2	-8.0 +8.6	-14.8 +16.0	(-9.0, +8.0) (+4.0, -4.0)	-7.0 +11.8
800	9.4	-9.7 +10.6	-19.3 +21.5	(-18.2, +18.2) (+6.1, -6.1)	-8.7 +9.5

giving $\gamma_{\text{H}} = 168.84(\text{LO}), 180.94(\text{NLO}), 186.59(\text{NNLO}) \text{ GeV}$ for $\mu_{\text{H}} = 700 \text{ GeV}$. Using the three known terms in the series we estimate a 68% credible interval of $\gamma_{\text{H}} = 186.59 \pm 1.93 \text{ GeV}$. The difference NNLO – LO is 17.8 GeV and in the full SM our estimate is $\gamma_{\text{H}} = 163.26 \pm 11.75 \text{ GeV}$. Therefore, using $\gamma_{\text{H}} (1 \pm \delta_{\text{H}})$ we can give a rough but reasonable estimate of the remaining uncertainty on the lineshape. Of course, one could plot the lineshape with an error band (an example is shown in Figure 6 for $\mu_{\text{H}} = 700 \text{ GeV}$) but it is better to quantify the uncertainty at the level of those quantities that characterize the resonance. Referring to Eq.(51) we introduce the following quantities:

$$\begin{aligned}
 \sigma^{\text{prod}} & \quad \text{total production cross-section} \\
 \Sigma = \frac{d\sigma^{\text{prod}}}{d\zeta} & \quad \text{differential distribution} \\
 \{\zeta_{\text{max}}, \Sigma_{\text{max}}\} & \quad \text{the maximum of the lineshape} \\
 \{\zeta_{\pm}, \frac{1}{2}\Sigma_{\text{max}}\} & \quad \text{the half-maxima of the lineshape} \\
 A = \int_{\zeta_{-}}^{\zeta_{+}} d\zeta \Sigma & \quad \text{the area of the resonance between half-maxima} \tag{86}
 \end{aligned}$$

where ζ is the Higgs virtuality. Changing γ_{H} to $1 \pm \delta_{\text{H}}$ gives a variation on the production cross-section which is linear in δ_{H} , as shown in Table 15; similarly, the variation in the peak height goes as $2\delta_{\text{H}}$ with no appreciable variation in its position, ζ_{max} . In Table 15 we also show the variation (in GeV) in the position of the half-maxima and in the area of the resonance.

To summarize our estimate of the theoretical uncertainty associated to the signal:

- the remaining uncertainty on the production cross-section is typically well reproduced by $(\delta_{\text{H}} + 1)[\%]$
- Σ_{max} changes approximately with the naive expectation, $2\delta_{\text{H}}[\%]$
- The shift induced in the position of the half-maxima are more complicated but a rough approximation is given by

$$\Delta\zeta_{\pm} \approx \pm \frac{1}{2} \frac{\mu_{\text{H}}}{M_{\pm}} \gamma_{\text{H}} \delta_{\text{H}}, \quad M_{\pm} = \mu_{\text{H}}^{1/2} (\mu_{\text{H}} \pm \gamma_{\text{H}})^{1/2}. \tag{87}$$

How to use these results depends on the specific analysis, $\text{H} \rightarrow \text{WW} \rightarrow \text{lvlv}, \text{lvqq}$ and $\text{H} \rightarrow \text{ZZ} \rightarrow \text{llll}$ etc. For example, the lineshape information is used in $\text{H} \rightarrow \text{WW} \rightarrow \text{lvqq}$ analysis [73]. The $\text{H} \rightarrow \text{ZZ} \rightarrow \text{llvv}$ analysis use transverse mass spectrum for the llvv system. If the analysis is a simple “counting experiment”, therefore not taking the Higgs lineshape into account, the uncertainty on the area and the half-maxima can be neglected. Therefore, informations on the shape of the resonance will become more relevant once more advanced analysis techniques (based on differential distributions as discriminant variable) will be used.

The factor $\Gamma_{\text{H}}^{\text{tot}}(\zeta)$ in Eq.(27) deserves a separate discussion. As explained in Section 4 it represents the “on-shell” decay of an Higgs boson of mass $\sqrt{\zeta}$ and we have to quantify the corresponding uncertainty. The starting point is Γ^{tot} computed by PROPHECY4F [47] which includes two-loop leading corrections in $G_{\text{F}}M_{\text{H}}^2$, where M_{H} is now the on-shell mass. Next we consider the on-shell width in the Higgs-Goldstone model,

Table 16: Theoretical uncertainty on the total decay width, $\Gamma_{\text{H}}^{\text{tot}}$ in Eq.(27). Γ_p is the total width computed by PROPHECY4F, $\Delta\Gamma$ gives the credible intervals and $\delta\Gamma[\%]$ is the ratio $\Delta\Gamma/\text{Gamma}_p$.

$\sqrt{\zeta}[\text{GeV}]$	$\Gamma_p[\text{GeV}]$	$\delta\Gamma[68\%]$	$\delta\Gamma[95\%]$
600	123	0.25	0.42
700	199	0.62	1.03
800	304	1.35	2.24
900	449	2.63	4.38
1000	647	4.72	7.85
1200	1205	13.1	21.7
1500	3380	34.7	57.8
2000	15800	98.9	165

discussed in Refs. [18,74]. We have

$$\frac{\Gamma_{\text{H}}}{\sqrt{\zeta}}\Big|_{HG} = \sum_{n=1}^3 a_n \lambda^n = X_{HG}, \quad \lambda = \frac{G_{\text{F}}\zeta}{2\sqrt{2}\pi^2}. \quad (88)$$

Let $\Gamma_p = X_p \sqrt{\zeta}$ the width computed by PROPHECY4F, we redefine the total width as

$$\frac{\Gamma_{\text{tot}}}{\sqrt{\zeta}} = (X_p - X_{HG}) + X_{HG} = \sum_{n=0}^3 a_n \lambda^n, \quad (89)$$

where now $a_0 = X_p - X_{HG}$. As long as λ is not too large we can define a $p\% < 80\%$ credible interval as (following from $a_{2,3} < a_1$)

$$\Gamma_{\text{tot}}(\zeta) = \Gamma_p(\zeta) \pm \Delta\Gamma, \quad \Delta\Gamma = \frac{5}{4} \max\{|a_0|, a_1\} p\% \lambda^4 \sqrt{\zeta}. \quad (90)$$

It is easily seen that for $\sqrt{\zeta} = 929 \text{ GeV}$ the two-loop corrections are of the same size of the one-loop corrections and for $\sqrt{\zeta} = 2.6 \text{ TeV}$ one-loop and Born become of the same size. Note that the expansion parameter in Eq.(88) is one for $\sqrt{\zeta} = 1.57 \text{ TeV}$. In Table 16 we present both the 68% and the 95% credible intervals. This should be compared with the corresponding estimate in Ref. [2] of 17% ($M_{\text{H}}^4/1 \text{ TeV}$) for $M_{\text{H}} > 500 \text{ GeV}$. Due to the large effect induced by radiative corrections for large values of M_{H} and to the fact that the two-loop correction is only known in the Higgs-Goldstone Lagrangian we have devoted Appendix B to a detailed discussion of the validity of the whole approach.

It is clear that it does not make much sense to have an error estimate beyond 1.3 TeV and, therefore, all results for the Higgs lineshape that have a sizable fraction of events in this high-mass region should not be taken too seriously. Here, once again, the only viable alternative to define the Higgs signal is the CPP-scheme.

To summarize: above 0.93 TeV perturbation theory becomes questionable since the two-loop corrections start to become larger than the one-loop ones; above 1.3 TeV the error estimate also becomes questionable since the expansion parameter is $\lambda = 0.7$ and the 95% credible interval (after inclusion of the leading two-loop effects) is 32.2%. The invariant mass distribution for $\mu_{\text{H}} = 800 \text{ GeV}$ and the corresponding uncertainty introduced by $\Gamma_{\text{tot}}(\zeta)$ are shown in Figure 7.

The theoretical uncertainties coming from γ_{H} and Γ_{tot} can be combined but a meaningful prediction requires that we cut the Higgs virtuality (ζ) at some upper value for which we have selected $\zeta_{\text{max}} = (1.5 \text{ TeV})^2$. Results are shown in Table 17 and in Table 18, otherwise the non-perturbative increasing of $\Gamma_{\text{tot}}(\zeta)$ overcompensates the decreasing of $\sigma_{ij \rightarrow \text{H}}$ with a negligible smearing from the invariant mass distribution. For completeness we present the leading (in the limit $M_{\text{H}}^2 \rightarrow \infty$) K -factor for the $\text{H} \rightarrow \text{VV}$ amplitude ($\text{V} = \text{W}, \text{Z}$)

Table 17: Total theoretical uncertainty on the production cross-section at 7 TeV . The total is obtained by considering the THU on γ_H and on Γ_{tot} with a cut $\sqrt{\zeta} < 1.5 TeV$.

μ_H [GeV]	$\delta\sigma^{\text{prod}}$ [%]
600	-5.5 +5.9
700	-7.0 +7.5
800	-7.7 +8.8
900	-7.0 +8.9

Table 18: Total theoretical uncertainty on the production cross-section at 8 TeV . The total is obtained by considering the THU on γ_H and on Γ_{tot} with a cut $\sqrt{\zeta} < 1.5 TeV$.

μ_H [GeV]	$\delta\sigma^{\text{prod}}$ [%]
600	-5.2 +5.8
700	-6.3 +7.4
800	-6.7 +8.4
900	-6.0 +8.1

in the OS-scheme and in the CPP-scheme:

$$\begin{aligned}
 \text{OS} \quad K &\sim 1 + a_1 \frac{G_F M_H^2}{16\sqrt{2}\pi^2} + a_2 \left(\frac{G_F M_H^2}{16\sqrt{2}\pi^2} \right)^2 \\
 \text{CPP} \quad K &\sim 1 + a_1 \frac{G_F s_H}{16\sqrt{2}\pi^2} + (a_2 + 3i\pi a_1) \left(\frac{G_F s_H}{16\sqrt{2}\pi^2} \right)^2,
 \end{aligned} \tag{91}$$

where the coefficients are [74]

$$a_1 = 1.40 - 11.35 i \quad a_2 = -34.41 - 21.00 i \tag{92}$$

Above 1 TeV the NNLO term dominates the K -factor.

7.1 Interference signal/background

The most important factor that has to be observed here is that our analysis of the residual theoretical uncertainty refers to the signal only. In the current experimental analysis there are additional sources of uncertainty, e.g. background and Higgs interference effects. As a matter of fact, this interference is partly available and should not be included as a theoretical uncertainty; for a discussion and results we refer to Refs. [49,50]. In particular, from Refs. [49] we see that at $\mu_H = 600 GeV$ (the highest value reported) the effect is about +40% in the window $\zeta = 440-560 GeV$, is practically zero at the peak and reaches -50% after $\zeta = 680 GeV$ (no cuts applied). For the total cross-section in $gg \rightarrow lv\bar{l}'v'$ at $\mu_H = 600 GeV$ the effect of including the interference is already +34% and rapidly increasing with μ_H .

We stress that setting limits without including the effects of the interference induces large variations in rate and shape that will propagate through to all distributions. Therefore, any attempt to analyze kinematic distributions which are far from the SM shape may result in misleading limits.

8 Conclusions

In the last two decades many theoretical studies lead to improved estimates of the SM Higgs boson total cross section at hadron colliders [75,76,51,77,78,79,80,81] (including electroweak NLO corrections [82,83])

and of Higgs boson partial decay widths [84,47]. Less work has been devoted to studying the Higgs boson invariant mass distribution (Higgs–boson-lineshape) [21,22,55].

In this work we made an attempt to resolve the problem by comparing different theoretical inputs to the off-shellness of the Higgs boson. There is no question at all that the zero-width approximation should be avoided, especially in the high-mass region where the on-shell width becomes of the same order as the on-shell mass, or higher.

The propagation of the off-shell H is usually parametrized in terms of some Breit-Wigner distribution; several variants are reported in the literature, e.g. Eq.(34) and Eq.(74), see Ref. [57] for a discussion. We have shown evidence that only the Dyson-resummed propagator should be used, leading to the introduction of the H complex pole, a gauge-invariant property of the S -matrix.

Finally, when one accepts the idea that the Higgs boson is an off-shell intermediate state the question of the most appropriate choice of QCD scales arises. We have shown the effect of including dynamical choices for QCD scales, μ_R, μ_F , instead of a static choice.

For many purposes the well-known and convenient machinery of the on-shell approach can be employed but one should become aware of its limitations and potential pitfalls. Although the basic comparison between different schemes was presented in this work, at this time we are repeating that differences should not be taken as the source of additional theoretical uncertainty; in Section 4 we have shown that the CPP-scheme, described in Section 3.1 (see Eq.(46)), is the only the only theoretically consistent tool for describing the lineshape; it requires, however, the computation of Feynmann diagrams on the second Riemann-sheet. As a consequence, our simple pragmatic recommendation is to use the OFFP-scheme described in Section 3.1 (see Eq.(45)) with running QCD scales. The associated theoretical uncertainty has been discussed in Section 7 where we also examine the limitations induced by an apparent breakdown of the perturbative expansion in the ultra-heavy Higgs boson limit.

Finally, the most severe problem faced by a critical appraisal of the heavy Higgs boson lineshape is the missing inclusion of interference with the background, especially in the light of gauge invariance issues.

Acknowledgments

We gratefully acknowledge several important discussions with C. Anastasiou, M. Cacciari, G. Carrillo, A. Denner, S. Dittmaier, S. Forte, S. Frixione, M. Grazzini, F. Maltoni, C. Mariotti, P. Nason, C. Oleari, S. Pozzorini, B. Quayle, D. Rebuzzi, M. Spira, C. Sturm, R. Tanaka and S. Uccirati. This work has been performed within the Higgs Cross-Section Working Group

<https://twiki.cern.ch/twiki/bin/view/LHCPhysics/CrossSections>.

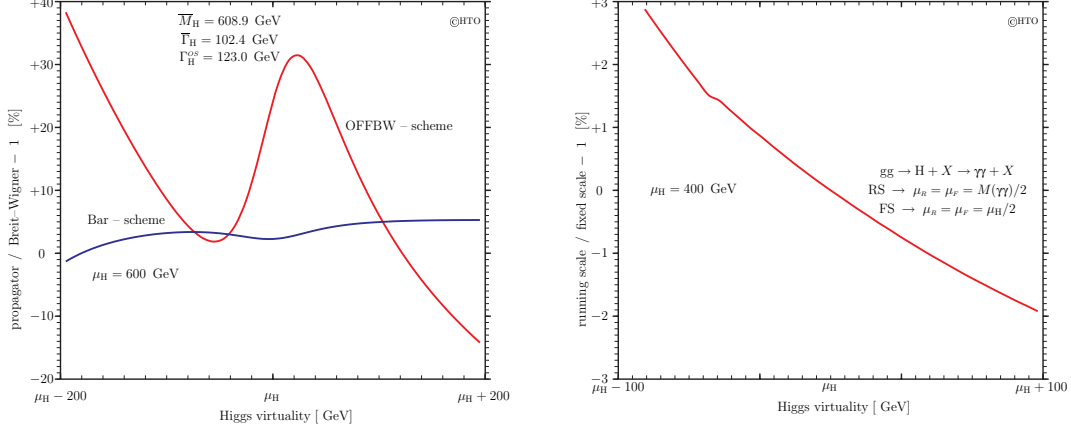


Figure 1: In the left figure we show a comparison of production cross-section as computed with the OFFBW-scheme of Eq.(45) or with the OFFBW-scheme of Eq.(43). The red curve gives Breit-Wigner parameters in the OS-scheme and the blue one in the Bar-scheme of Eq.(36). In the right figure we show the effect of using dynamical QCD scales for the production cross-section of Eqs.(51)–(53).

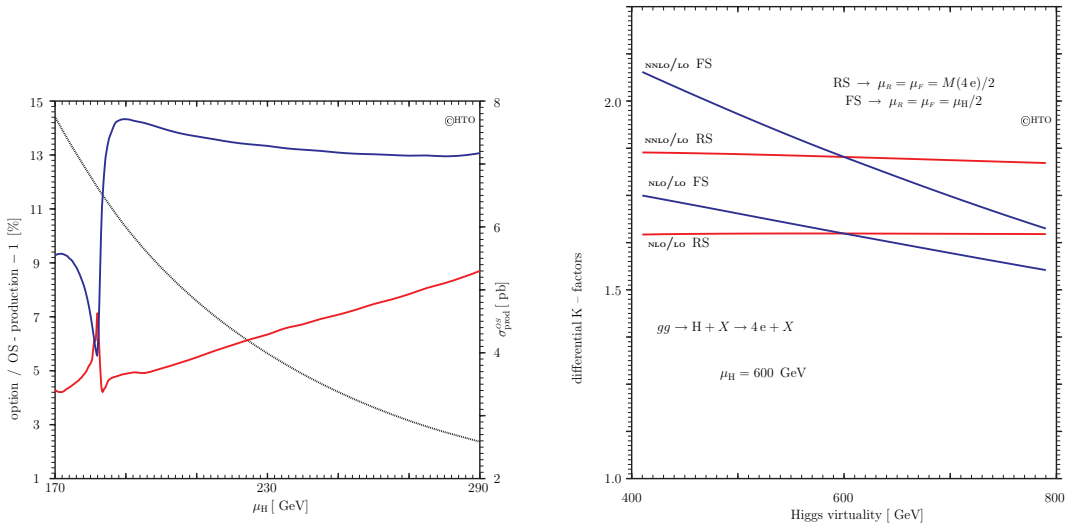


Figure 2: In the left figure the blue curve gives the off-shell production cross-section sampled over the (complex) Higgs propagator while the red curves is sampled over a Breit-Wigner distribution. The black curve gives the on-shell production cross-section. The right figure shows differential K factor for the process $pp \rightarrow (H \rightarrow 4e) + X$, comparing the fixed scale option, $\mu_R = \mu_F = M_H/2$, and the running scale option, $\mu_R = \mu_F = M(4e)/2$.

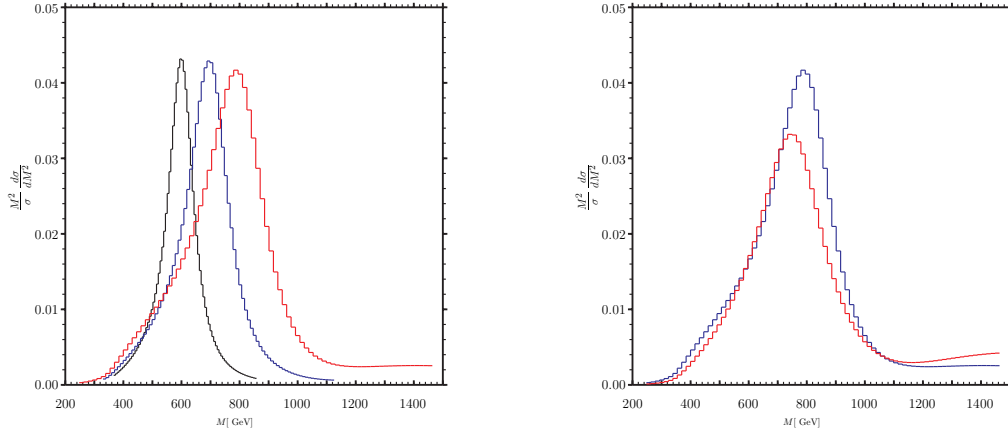


Figure 3: The normalized invariant mass distribution in the OFFFP-scheme with running QCD scales (left) for 600 *GeV* (black), 700 *GeV* (blue), 800 *GeV* (red) in the windows $M_{\text{peak}} \pm 2\Gamma_{\text{OS}}$. The normalized invariant mass distribution in the OFFFP-scheme (blue) and OFFBW-scheme (red) with running QCD scales (right) at 800 *GeV* in the window $M_{\text{peak}} \pm 2\Gamma_{\text{OS}}$.

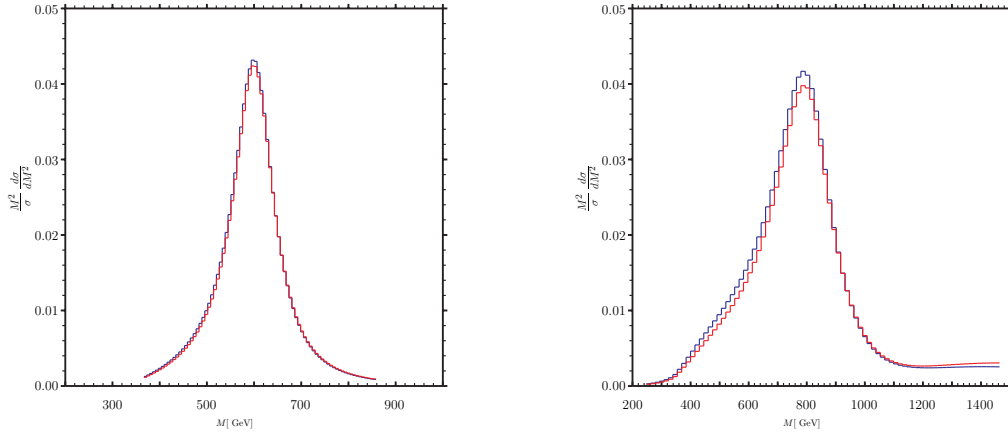


Figure 4: The normalized invariant mass distribution in the OFFFP-scheme with running QCD scales for 600 *GeV* (left), 800 *GeV* (right) in the windows $M_{\text{peak}} \pm 2\Gamma_{\text{OS}}$. The blue line refers to 8 *TeV*, the red one to 7 *TeV*.

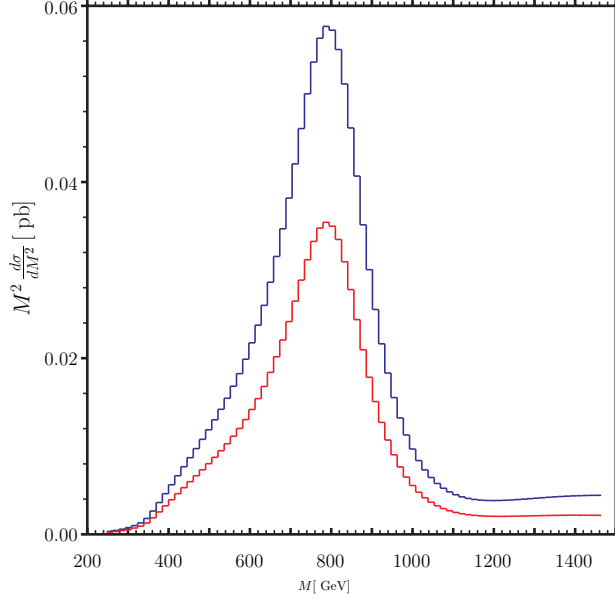


Figure 5: The invariant mass distribution in the OFFP-scheme with running QCD scales for 800 GeV in the window $M_{\text{peak}} \pm 2\Gamma_{\text{OS}}$. The blue line refers to 8 TeV , the red one to 7 TeV .

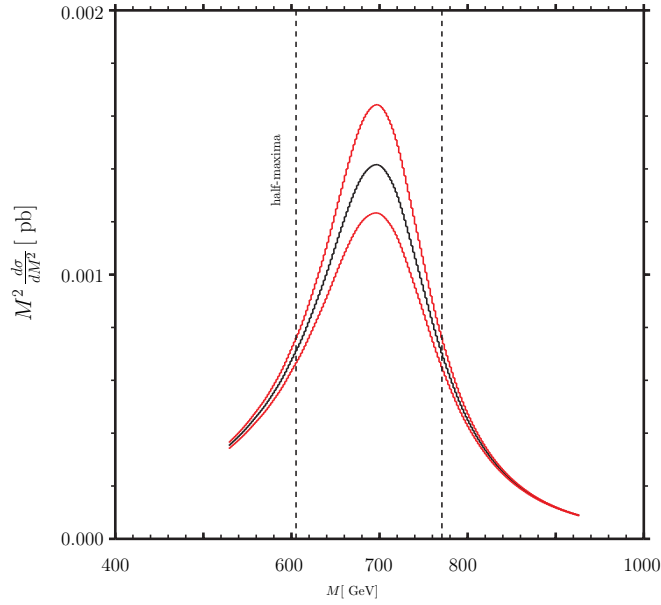


Figure 6: The invariant mass distribution in the OFFP-scheme with running QCD scales for $\mu_{\text{H}} = 700 \text{ GeV}$ in the window $M_{\text{peak}} \pm \Gamma_{\text{OS}}$. The red lines give the associated theoretical uncertainty as discussed in Section 7.

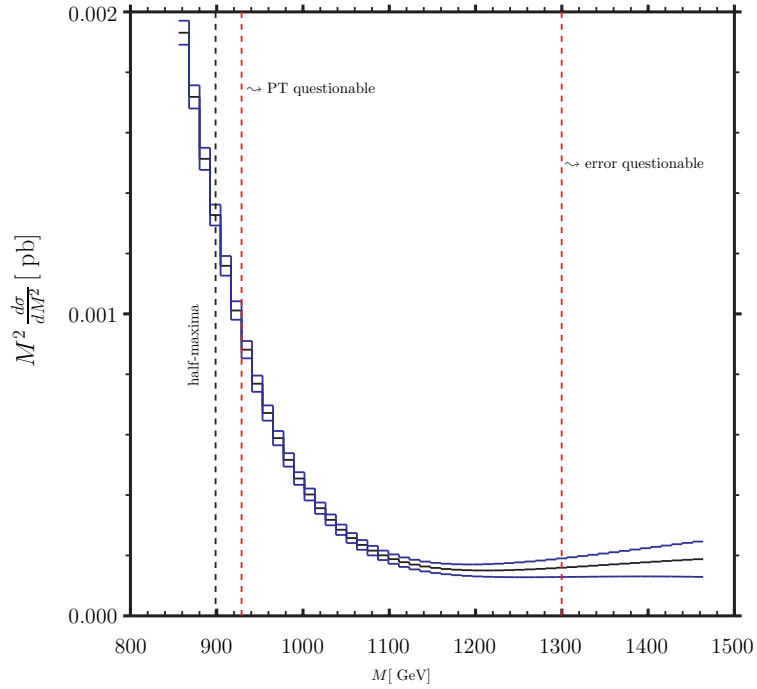


Figure 7: The invariant mass distribution in the OFFP-scheme for $\mu_H = 800 \text{ GeV}$ in the window $[M_{\text{peak}} - M_{\text{peak}} + 2\Gamma_{\text{OS}}]$ with the error band due to the theoretical uncertainty introduced by $\Gamma_H^{\text{tot}}(\zeta)$ discussed in Section 7.

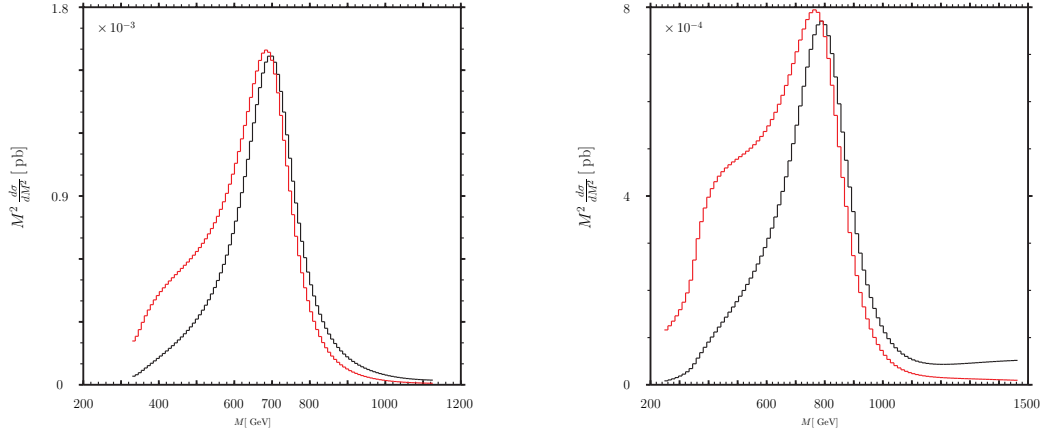
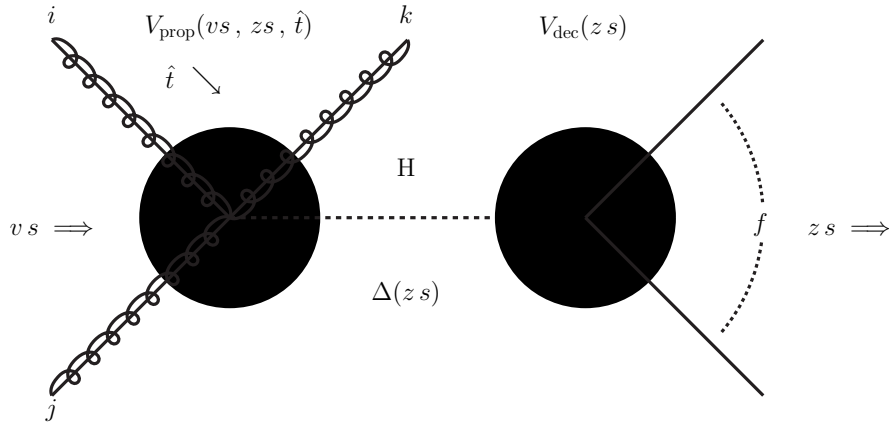


Figure 8: The invariant mass distribution in the OFFP-scheme (black) and in the CPP-scheme (red) for $\mu_H = 700 \text{ GeV}$ (left) and $\mu_H = 800 \text{ GeV}$ (right) in the window $[M_{\text{peak}} - 2\Gamma_{0S} - M_{\text{peak}} + 2\Gamma_{0S}]$ for the process $gg \rightarrow H \rightarrow Z^c Z^c$.



$$\begin{aligned}
&\Rightarrow \sigma_{ij \rightarrow H+k}(v_s, \hat{t}, z_s) \frac{v z s^2}{|z s - s_H|^2} \frac{\Gamma_{H \rightarrow f}(z s)}{(z s)^{1/2}} + \text{NR} \\
&= \sigma_{ij \rightarrow H+k}(v_s, \hat{t}, s_H) \frac{v s |s_H|^{1/2}}{|z s - s_H|^2} \Gamma_{H \rightarrow f}(s_H) + \text{NR}'
\end{aligned}$$

Figure 9: The resonant part of the process $ij \rightarrow H+k$ where i, j and k are partons (g or q). We distinguish between production, propagation and decay, indicating the explicit dependence on Mandelstam invariants. If s denotes the pp invariant mass we distinguish between $v s$, the ij invariant mass, $z s$, the Higgs boson virtuality and \hat{t} which is related to the Higgs boson transverse momentum. Within NR we include the Non-Resonant contributions as well as their interference with the signal. NR' includes those terms that are of higher order in the Laurent expansion of the signal around the complex pole. At NNLO QCD the parton k is a pair k_1-k_2 and more invariants are needed to characterize the production mechanism.

A Appendix: Nielsen identities at work

In this Appendix we consider one specific example of application of Nielsen identities (see Ref. [61]) at one loop level, namely we explain of to get gauge-parameter independence in the process

$$H(P) \rightarrow Z(p_1, \mu) + Z(p_2, \nu). \quad (93)$$

We work in the R_ξ -gauge; for any quantity $f(\xi)$ we write a decomposition

$$f(\xi) = f(1) + \Delta f(\xi), \quad \Delta f(1) = 0. \quad (94)$$

The most important quantity is the Higgs self-energy,

$$S_{\text{HH}}(s) = S_{\text{HH}}^{(1)} + \mathcal{O}(g^4) = \frac{g^2}{16\pi^2} \Sigma_{\text{HH}}(s) + \mathcal{O}(g^4), \quad s = -P^2. \quad (95)$$

Let M_{H} be the renormalized Higgs mass, we obtain that the one-loop, ξ -dependent, part can be given as

$$\Delta \Sigma_{\text{HH}}^{(1)}(\xi, s, M_{\text{H}}^2) = (s - M_{\text{H}}^2) \sigma_{\text{HH}}^{(1)}(\xi, s, M_{\text{H}}^2). \quad (96)$$

The main equation is the one for the Higgs complex pole,

$$s_{\text{H}} - M_{\text{H}}^2 + S_{\text{HH}}^{(1)}(\xi, s_{\text{H}}, M_{\text{H}}^2) = 0, \quad (97)$$

from wick we derive

$$M_{\text{H}}^2 = s_{\text{H}} + \mathcal{O}(g^2), \quad \frac{\partial}{\partial \xi} S_{\text{HH}}^{(1)}(\xi, s_{\text{H}}, s_{\text{H}}) = 0. \quad (98)$$

Next we consider the one-loop vertices contributing to $H \rightarrow ZZ$ and obtain a one-loop amplitude

$$A_{\text{V}}^{(1)}(H \rightarrow ZZ) = (V_{\text{d}}^{(1)} \delta_{\mu\nu} + V_{\text{p}}^{(1)} p_{2\mu} p_{1\nu}) e^\mu(p_1, \lambda_1) e^\nu(p_2, \lambda_2). \quad (99)$$

Using the decomposition

$$V_{\text{d,p}}^{(1)}(\xi, s, M_{\text{H}}^2) = V_{\text{d,p}}^{(1)}(1, s, M_{\text{H}}^2) + \Delta V_{\text{d,p}}^{(1)}(\xi, s, M_{\text{H}}^2) \quad (100)$$

we obtain the following results:

1. after reduction to scalar form-factors there are no scalar vertices remaining in $\Delta V_{\text{d}}^{(1)}(\xi, s_{\text{H}}, s_{\text{H}})$.
2. Furthermore, $\Delta V_{\text{p}}^{(1)}(\xi, s_{\text{H}}, s_{\text{H}}) = 0$.

Both results are expected since the corresponding terms could not cancel against anything else. Furthermore we compute renormalization Z-factors for the external legs [53]

$$\begin{aligned} s - M_{\text{H}}^2 + S_{\text{HH}}^{(1)}(\xi, s, M_{\text{H}}^2) &= (s - s_{\text{H}}) \left[1 + \frac{S_{\text{HH}}^{(1)}(\xi, s, s_{\text{H}}) - S_{\text{HH}}^{(1)}(\xi, s_{\text{H}}, s_{\text{H}})}{s - s_{\text{H}}} \right] \\ &= (1 + Z_{\text{H}}) (s - s_{\text{H}}) + \mathcal{O}\left((s - s_{\text{H}})^2\right). \end{aligned} \quad (101)$$

It follows that

$$\Delta V_{\text{d}}^{(1)}(\xi, s_{\text{H}}, s_{\text{H}}) - \left[\frac{1}{2} \Delta Z_{\text{H}}(\xi) + \Delta Z_{\text{Z}}(\xi) \right] A^{(0)} = 0, \quad (102)$$

where the lowest-order is defined by

$$A^{(0)} = -g \frac{M_{\text{W}}}{\cos^2 \theta}, \quad \cos^2 \theta = \frac{M_{\text{W}}^2}{M_{\text{Z}}^2}, \quad M_{\text{W,Z}}^2 = s_{\text{W,Z}}. \quad (103)$$

At one loop it is enough to evaluate all functions at $s = M_{\text{H}}^2$ but only s_{H} is ξ -independent.

B Appendix: equivalence theorem for (off-shell) virtual bosons

In this Appendix we discuss the extension of the equivalence theorem to virtual vector-bosons. Formally, the theorem states, at the S -matrix level, that

$$S[\mathbb{V}_L] = (iC)^n S[\phi], \quad (104)$$

where n is the number of external, longitudinal, vector-bosons and $C = 1$ at tree level. In Ref. [85] it is shown how one can get $C = 1$ at higher orders through a choice of the ϕ renormalization constant. We consider the amplitude for the process

$$H(P) \rightarrow \bar{f}(q_1) + f(k_1) + \bar{f}(q_2) + f(k_2), \quad (105)$$

where all fermion are massless. The amplitude can be split according to the number of resonant vector-bosons,

$$A = A_{2V} + A_{1V} + A_{0V}, \quad (106)$$

where A_{2V} starts from LO in perturbation theory while A_{1V}, A_{0V} start from NLO. Furthermore we have

$$A_{2V} = [F_d \delta^{\mu\nu} + F_p \frac{p_1^\mu p_2^\nu}{M_H^2}] \Delta_{\mu\alpha}^V(p_1) \Delta_{\nu\beta}^V(p_2) J^\alpha(q_1, k_1) J^\beta(q_2, k_2), \quad (107)$$

where Δ_V is the vector-boson propagator and $J^{\alpha,\beta}$ are (conserved) fermion currents. In the $\xi = 1$ gauge there are no scalar propagators involved and each V-propagator is proportional to $\delta_{\mu\alpha}$ etc.

We are interested in the leading term of the amplitude in the limit $M_H \rightarrow \infty$. This term derives from a balance between $H\phi$ -couplings (ϕ stands for a generic Goldstone-boson) and H-propagators; at one-loop (or higher) A_{1V} is given by boxes and A_{1V} by pentagons. Since external fermions are massless we can easily see that there are not enough internal scalars to contribute to the leading term.

We will use the formalism of Refs. [86,87,88] and will write

$$\delta_{\mu\nu} - \frac{p_\mu p_\nu}{p^2} = e_{L\mu}(p) e_{L\nu}^*(p) + \sum_{\lambda=-1,+1} e_{\perp\mu}(p, \lambda) e_{\perp\nu}^*(p, \lambda). \quad (108)$$

Since the fermion currents are conserved we can replace the numerator in the V-propagators with the sum over polarizations. A convenient choice for the polarizations is the following:

$$e_{L\mu}(p_1) = -N_L^1 (p_1 \cdot p_2 p_{1\mu} + s_1 p_{2\mu}), \quad e_{L\mu}(p_2) = -N_L^2 (p_1 \cdot p_2 p_{2\mu} + s_2 p_{1\mu}), \quad (109)$$

where $N_{1,2}$ are the normalizations, $p_i^2 = -s_i$ and

$$e_{\perp\mu}(p_i, \lambda) = \frac{1}{\sqrt{2}} [n_\mu(p_i) + i\lambda N_\mu(p_i)], \quad N_\mu(p_i) = (s_i)^{-1/2} \varepsilon_{\mu\alpha\beta\rho} n^\alpha(p_i) e_L^\beta(p_i) p_i^\rho, \quad (110)$$

$$n_\mu(p_1) = i N_\perp^1 \varepsilon_{\mu\alpha\beta\rho} k_1^\alpha p_1^\beta p_2^\rho, \quad n_\mu(p_2) = i N_\perp^2 \varepsilon_{\mu\alpha\beta\rho} k_2^\alpha p_2^\beta p_1^\rho. \quad (111)$$

With this choice one obtains

$$\sum_{\lambda=-1,+1} e_{\perp\mu}(p, \lambda) e_{\perp\nu}^*(p, \lambda) = \delta_{\mu\nu} - \frac{p_\mu p_\nu}{p^2} - e_{L\mu}(p) e_{L\nu}^*(p). \quad (112)$$

The first question to answer is about L -polarization dominance in Higgs decay for $M_H \rightarrow \infty$ ⁵. For the F_d, F_p parts in Eq.(107) we have to evaluate

$$\sum_{\lambda_1, \lambda_2} e(p_1 \lambda_1) \cdot e(p_2 \lambda_2) e_\alpha^*(p_1, \lambda_1) e_\beta^*(p_2, \lambda_2),$$

⁵We gratefully acknowledge A. Denner and S. Dittmaier for an important discussion on this point.

$$\sum_{\lambda_1, \lambda_2} e(p_1, \lambda_1) \cdot p_2 e(p_2, \lambda_2) \cdot p_1 e_\alpha^*(p_1, \lambda_1) e_\beta^*(p_2, \lambda_2). \quad (113)$$

First we introduce invariants for the complete process

$$\begin{aligned} q_1 \cdot k_1 &= -\frac{1}{2} s_1, & q_2 \cdot k_2 &= -\frac{1}{2} s_2, & q_1 \cdot q_2 &= -\frac{1}{2} s_3, \\ q_1 \cdot k_2 &= -\frac{1}{2} s_4, & k_1 \cdot q_2 &= -\frac{1}{2} s_5, & k_1 \cdot k_2 &= -\frac{1}{2} s_6, \end{aligned} \quad (114)$$

where the invariants satisfy $\sum_i s_i = M_H^2$. Therefore, not all scales in the problem can be small as compared to M_H^2 . For the V squared-propagators we have

$$\frac{1}{(s - M_V^2)^2 + \Gamma_V^2 M_V^2} = \frac{\pi}{M_V \Gamma_V} \delta(s - M_V^2) + \text{PV} \left[\frac{1}{(s - M_V^2)^2} \right] + \dots \quad (115)$$

Therefore, always in the limit $M_H \rightarrow \infty$, we can assume that $s_{1,2} \approx M_V^2 \rightarrow 0$. In the rest-frame of the Higgs boson and using massless fermions in the final state, the condition $s_{1,2} = 0$ requires $s_i = M_H^2/4$ for $i = 3, \dots, 6$. Next we introduce

$$D_{L;L} = \left| e_L(p_1) \cdot e_L(p_2) \right|^2, \quad D_{\perp-; \perp-} = \left| e_\perp(p_1, -1) \cdot e_\perp(p_2, -1) \right|^2, \quad (116)$$

etc. in the limit $s_{1,2} \rightarrow 0$ and $M_H \rightarrow \infty$. We obtain

$$D_{L;L} = \frac{1}{4} \frac{M_H^4}{s_1 s_2} - \frac{1}{2} \frac{s_1 + s_2}{s_1 s_2} M_H^2 + \mathcal{O}(1), \quad (117)$$

while all other combinations are finite in the limit. We also introduce non-diagonal elements,

$$N_{\lambda\sigma\rho\tau} = e(p_1, \lambda) \cdot e(p_2, \sigma) \left[e(p_1, \rho) \cdot e(p_2, \tau) \right]^*, \quad (118)$$

where $e(p, 0) = e_L(p)$ and $e(p, \pm 1) = e_\perp(p, \pm 1)$. Also these elements are finite or zero in the limit $s_1, s_2 \rightarrow 0$. Furthermore, we introduce other quantities

$$P_{L;L} = \left| e_L(p_1) \cdot p_2 e_L(p_2) \cdot p_1 \right|^2, \quad (119)$$

etc. (including non-diagonal terms) and find

$$P_{L;L} = \frac{1}{16} \frac{M_H^8}{s_1 s_2} - \frac{1}{4} \frac{s_1 + s_2}{s_1 s_2} M_H^6 + \mathcal{O}(M_H^4), \quad (120)$$

while all other combinations are finite in the limit. Finally we define the fermion part of the amplitude, squared and summed over spins:

$$\Gamma_L = \sum_{\text{spins}} \left| J(q, k) \cdot e_L(p) \right|^2, \quad \Gamma_{\perp; \lambda} = \sum_{\text{spins}} \left| J(q, k) \cdot e_\perp(p, \lambda) \right|^2, \quad (121)$$

where $p = q + k$ and

$$J^\mu(q, k) = \bar{u}(k) \gamma^\mu (V_+ \gamma_+ + V_- \gamma_-) v(q), \quad \gamma_\pm = 1 \pm \gamma^5. \quad (122)$$

We obtain

$$\Gamma_L = 4 (V_+^2 + V_-^2) s + \mathcal{O}(s^2) \quad \Gamma_{\perp; \lambda} = 4 (V_+^2 + V_-^2) s + \mathcal{O}(s^2), \quad (123)$$

where $s = -p^2$. We also compute non-diagonal elements

$$\Gamma_{\lambda,\sigma} = \sum_{\text{spins}} J(q,k) \cdot e(p,\lambda) [J(q,k) \cdot e(p,\sigma)]^\dagger, \quad (124)$$

and find

$$\Gamma_{0,\pm 1} = 2\sqrt{2}i(V_+^2 - V_-^2)s + \mathcal{O}(s^2), \quad \Gamma_{-1,+1} = 2(V_+^2 + V_-^2)s + \mathcal{O}(s^2). \quad (125)$$

Therefore, all Γ factors are suppressed in the low- s region and, according to Eqs.(117)–(120), only longitudinal vector bosons contribute to the leading term for $M_H \rightarrow \infty$. In conclusion, for the double-resonant part of the amplitude, only the longitudinal polarizations matter. One-loop corrections are computed exactly in Ref. [47] which also includes two-loop leading corrections; they are extracted from the Higgs-Goldstone model and PROPHECY4F multiplies the complete LO width with the NNLO correction factor. For the contributions of the transverse vector-bosons it is not correct but irrelevant in the limit $M_H \rightarrow \infty$, as we have explicitly shown.

Before concluding our argument we need to explain how the equivalence theorem (see Ref. [85]) works in practice for our off-shell vector bosons. The theorem is based on a Ward-Slavnov-Taylor identity which relates the amplitude for a V-boson contracted with its momentum to the corresponding amplitude where the V-boson is replaced by a Goldstone-boson ϕ . However, in our case we have

$$e_{L\mu}(p_1) = -N_L^1(p_1 \cdot p_2 p_{1\mu} + s_1 p_{2\mu}), \quad (126)$$

and the longitudinal polarization is not simply proportional to the momentum. To see how it works in the $M_H \rightarrow \infty$ limit, we consider the LO HW^+W^- vertex contracted with longitudinal polarizations

$$V_{L;L} = -g M_W e_L(p_1) \cdot e_L(p_2), \quad e_{L\mu}(p_1) = -N_L^1(L p_1 \cdot p_2 p_{1\mu} + R s_1 p_{2\mu}), \quad (127)$$

where we have artificially introduced the L, R coefficients. It is easy to show that only the L^2 part of $V_{L;L}$ survives in the limit, giving

$$V_{L;L} \sim \frac{1}{2} g \frac{M_W}{\sqrt{s_1 s_2}} M_H^2, \quad (128)$$

which, after identification of s_i with M_W^2 is exactly minus the $H\phi^+\phi^-$ vertex, as dictated by the equivalence theorem (but only in the limit $M_H \rightarrow \infty$). As expected, the WSTI relating $\partial_\mu V^\mu$ to $M_V \phi$, is valid only for on-shell particles. The same holds for the combination

$$-g M_W e_L(p_1) \cdot p_2 e_L(p_2) \cdot p_1, \quad (129)$$

showing that, in the limit $M_H^2 \rightarrow \infty$, we can extract the leading behavior from the Higgs-Goldstone model and we can multiply the LO width with the NNLO correction factor, channel-by-channel. The only delicate point concerns the WSTI which substitutes two (contracted) V-lines with ϕ lines. When only one of the two is contracted and the other is multiplied by the wrong momentum there is an additional term in the WSTI. We illustrate this singly-contracted WSTI at LO in Figure 10: if the J -source is physical ($p_2^\mu \cdot J_\mu(p_2) = 0$) then the sum of the first two diagrams is zero, otherwise there is a remainder given by diagram c) of Figure 10 where Faddeev-Popov ghosts are involved. A similar situation happens also at higher orders, as shown in Figure 11, where the dash-arrow line represents Faddeev-Popov ghosts and the off-shell V-source contracted with the wrong momentum can absorb a V-ghost pair. One can argue, on the basis of the explicit calculation, that this term is never leading at one-loop but we have not found a convincing argument that this is the case to all orders.

The above arguments, strictly speaking, apply to the decay of an on-shell Higgs boson. If this decay is part of a complete process, e.g. $gg \rightarrow 4f$ (where we have Higgs-resonant diagrams) then the following happens: let g be the $SU(2)$ coupling constant and $\lambda = g^2 M_H^2/M_W^2$; the work of Ref. [85] shows that, for $g^2/\lambda \rightarrow 0$, the equivalence theorem is true to lowest nonzero order in g and to all orders in λ . However, there is no reason to expect the theorem to hold when using a propagator with a Breit-Wigner width, which is equivalent to summing a subset of diagrams of higher order in λ .

We conclude the Appendix with another comment: technically speaking Eq.(104) requires that $S[\phi]$ is computed in the full SM, not only in the Higgs-Goldstone model. We have verified in simple examples that the difference is subleading when $M_H \rightarrow \infty$.

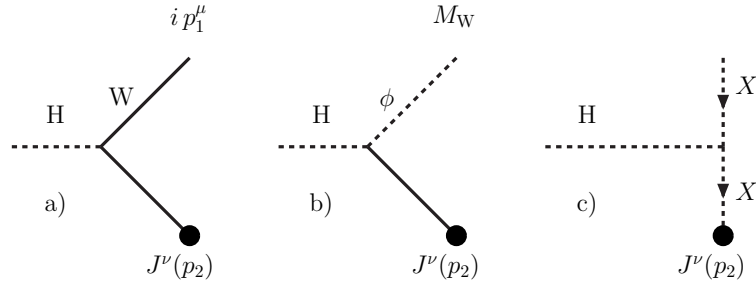


Figure 10: Example of a LO simply-contracted WSTI where the dash-line represents the Higgs boson, solid line represent vector-bosons and dash-arrow-lines represent Goldstone-bosons or Faddeev-Popov ghosts. If the source J is physical then $a + b = c = 0$, otherwise $a + b + c = 0$

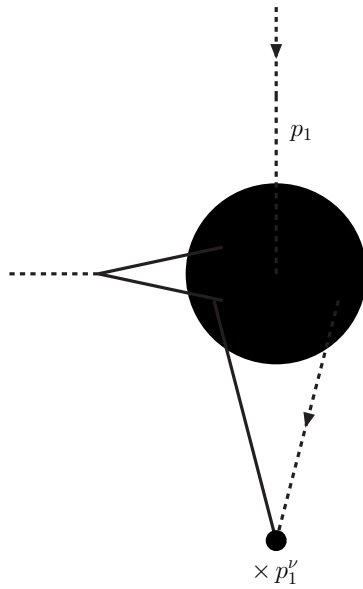


Figure 11: Example of a remainder for a NLO simply-contracted WSTI where the dash-line represents the Higgs boson, solid line represent vector-bosons and dash-arrow-lines represent Faddeev-Popov ghosts.

C Appendix: complex poles, real kinematics and pseudo-observables

In this Appendix we discuss how to implement complex poles in the amplitude for $H \rightarrow F$ within the CPP-scheme. For sake of simplicity we consider the process $H(P) \rightarrow Z(p_1) + Z(p_2)$ where both Z s are on-shell while the Higgs boson is off-shell, i.e. $P^2 = -s$. At LO the S -matrix element is

$$S_{\text{LO}} = -g \frac{M_Z}{\cos\theta} e(p_1) \cdot e(p_2). \quad (130)$$

Squaring the amplitude and summing over polarization introduces a P^2 which is a kinematic factor and should be replaced with s

$$\sum_{\text{spins}} \left| S_{\text{LO}} \right|^2 = \sqrt{2} G_{\text{F}} s^2 (1 - 4x_Z + 12x_Z^2), \quad x_Z = \frac{M_Z^2}{s}. \quad (131)$$

At LO there is never a problem with gauge parameter dependence. At NLO there is an amplitude

$$A_{\text{NLO}}^{\mu\nu} \left(s, M_{\text{H}}^2 \right) = s F_d \left(s, M_{\text{H}}^2 \right) \delta^{\mu\nu} + F_p \left(s, M_{\text{H}}^2 \right) p_1^\nu p_2^\mu, \quad (132)$$

where the M_{H}^2 arises from vertices and propagators, always with $P^2 = -s$. Renormalization in the complex-mass scheme requires the replacement $M_{\text{H}}^2 \rightarrow s_{\text{H}}$; taking the residue at the complex pole also requires $s \rightarrow s_{\text{H}}$ and guarantees gauge parameter independence. When we go to the S matrix element and compute the NLO correction we obtain

$$2 \operatorname{Re} \sum_{\text{spins}} S_{\text{LO}}^\dagger S_{\text{NLO}} = -144 (\sqrt{2} G_{\text{F}})^{3/2} M_{\text{W}} s^2 \left[x_Z \frac{\operatorname{Re} s_{\text{H}} F_d}{s} + \frac{1}{12} \left(1 - \frac{1}{6} \frac{1}{x_Z} + \frac{4}{3} x_Z \right) \operatorname{Re} F_p \right], \quad (133)$$

where the form factors are computed at $s = M_{\text{H}}^2 = s_{\text{H}}$. When there are more particles in the final state the analytical continuation of the form factors should be done according to Eqs.(48)–(49) and generalizations, followed by the integration over the phase space with real angles and energies.

C.1 Analytic continuation

We continue this Appendix emphasizing, yet once more, that complex kinematics is not needed since we need to perform analytic continuation in the S -matrix element (because of gauge invariance) while keeping the phase-space real; this is the approach introduced in Ref. [89], the so-called leading-pole-approximation (LPA). In Appendix A of Ref. [52] it is shown that, in order to have a pole on the second Riemann sheet independently of the other momentum variables, analytic continuation of the scattering amplitude in the variable k^0 is required (k being the momentum of the unstable particle). Therefore the S -matrix has to be analytically continued in k^0 around the positive energy cut to the second sheet and the state vector for the corresponding unstable particle must not depend on k^0 ; QFT provides an explicit construction for this state as described in details in Ref. [52].

Consider the process where an off-shell Higgs boson of virtuality $\sqrt{\zeta}$ decays into n massless particles of momentum q_i ; then the quantity of interest is

$$\begin{aligned} \Gamma_{H \rightarrow n}(\zeta) &= \frac{1}{2\sqrt{\zeta}} \int d\Phi_{1 \rightarrow n} \sum_{s,c} \left| A_{H \rightarrow n}(\{q_i \cdot q_j\}) \right|^2 \\ &= \frac{1}{2\sqrt{\zeta}} \int d\mathbb{I}_{3n-7} \sum_{s,c} \left| A_{H \rightarrow n}(\{I\}) \right|^2, \end{aligned} \quad (134)$$

where $\{I\}$ is the set of $3n - 7$ invariants, linearly independent, needed to describe the process. Another quantity of interest is the production cross-section for an off-shell Higgs boson plus jets, e.g. $g(p_1) + g(p_2) \rightarrow g(q_1) + H(q_2)$, with $q_2^2 = \zeta$,

$$\sigma_{gg \rightarrow H+nPg}(\zeta) = \frac{1}{2s} \int d\Phi_{2 \rightarrow n+1} \sum_{s,c} \left| A_{gg \rightarrow H+nPg}(\{q_i \cdot q_j\}) \right|^2$$

$$= \frac{1}{2s} \int d\mathbb{I}_{3n-1} \sum_{s,c} \left| A_{gg \rightarrow H+n g}(\{I\}) \right|^2, \quad (135)$$

An extension to complex kinematics is possible and the relevant work can be found in Ref. [52]; here we repeat the construction for completeness. We consider distortions of the original real contour that project one-to-one onto the original contour under the projection that sends complex momentum onto its real part. The contour of integration may be distorted in any bounded region provided the integrand is analytic through the region of distortion.

Suppose that, in a given process, k_c is the momentum of an unstable (incoming or outgoing) Higgs particle and k is its projection back to the real axis; the general form of k_c will be (here we work in the Bjorken-Drell metric)

$$\begin{aligned} k_c^\mu &= p^\mu + i q^\mu, & k_c^2 &= \mu_H^2 - i \mu_H \gamma_H = \hat{\mu}_H^2, \\ \hat{\mu}_H &= \frac{1}{\sqrt{2}} \mu_H \left(1 + \frac{\overline{M}_H}{M_H} \right)^{1/2} - \frac{i}{\sqrt{2}} \gamma_H \left(1 + \frac{\overline{M}_H}{M_H} \right)^{-1/2}. \end{aligned} \quad (136)$$

The vectors p, q must satisfy

$$p^2 - q^2 = \mu_H^2, \quad p \cdot q = -\frac{1}{2} \mu_H \gamma_H. \quad (137)$$

To have a resonance k must be a timelike momentum and we can go to a frame $k = (\sqrt{\zeta}, \vec{0})$ where ζ is the Higgs virtuality. We have chosen the following analytic continuation, yielding the complex pole:

$$\text{Step 1) } k_\zeta = L(k_\zeta, k) k, \quad k_\zeta = (\sqrt{\zeta}, \vec{0}), \quad (138)$$

where L is a Lorentz boost;

$$\text{Step 2) } k_\zeta \rightarrow k_M = (\mu_H, \vec{0}), \quad (139)$$

where the analytic continuation is defined by

$$k_\lambda = \frac{1}{2\sqrt{\zeta}} \left((2-\lambda)\zeta + \lambda\mu_H^2, 0, 0, 2\lambda(\mu_H^2 - \zeta) \right), \quad 0 \leq \lambda \leq 1. \quad (140)$$

Finally, we boost back in the \vec{k} direction and continue into the complex plane as follows:

$$\text{Step 3) } \rightarrow k_c = p + i q, \quad p = (\text{Re } k_c^0, \vec{k}), \quad q = (\text{Im } k_c^0, \vec{0}). \quad (141)$$

The continuation in Eqs.(138)–(139) is the real, on-shell, projection in LPA. Since $q^2 > 0$ from Eq.(137) it follows that $p^2 > 0$. Any such state may be transformed by a real Lorentz transformation into one with standard momentum \vec{k} defined by

$$\vec{p} = \left(\frac{p \cdot q}{\sqrt{q^2}}, 0, 0, \sqrt{\frac{G(p, q)}{q^2}} \right), \quad \vec{q} = (\sqrt{q^2}, \vec{0}), \quad (142)$$

where $G(p, q) = p^2 q^2 - (p \cdot q)^2$ is the Gram determinant of p, q .

Once complex boosts are allowed states with momentum k_c satisfying $k_c^2 = \hat{\mu}_H^2$ can be constructed from Eq.(142). However, states appearing in scattering processes have a timelike momentum. Therefore, the only unstable particle states that appear in physical processes have a momentum k_c that becomes timelike when continued back to the real axis, i.e. $p^2 > 0$ is needed to produce resonances while the associated q is not constrained. In the additional two cases we have standard momenta (i.e. in each case k_c is related by a real Lorentz transformation to the standard momentum \vec{k})

$$q^2 = 0, \quad \vec{p} = \left(\frac{\lambda^2 p^2 + (p \cdot q)^2}{2\lambda p \cdot q}, 0, 0, \frac{\lambda^2 p^2 - (p \cdot q)^2}{2\lambda p \cdot q} \right), \quad \vec{q} = (\lambda, 0, 0, \lambda),$$

$$q^2 < 0, \quad \bar{p} = \left(\sqrt{\frac{G(p, q)}{q^2}}, 0, 0, \frac{p \cdot q}{\sqrt{-q^2}} \right) \quad \bar{q} = (\vec{0}, \sqrt{-q^2}). \quad (143)$$

The possibility of having two parametrizations connected by a complex boost (an element of $L(\mathbb{C})$ the complex, homogeneous Lorentz group) may seem like posing a question of uniqueness, but it does not since scalar products are defined without complex conjugation of one of the complex four-vectors.

Since we perform our analytic continuation on the invariants (see Eqs.(134)–(135)) we have to define the mapping. Consider again the process $g(p_1) + g(p_2) \rightarrow g(k_1) + H(k_2)$ and define $s = (p_1 + p_2)^2$, $t = (p_1 - k_2)^2$ and

$$t = -\frac{s}{2} \left(1 - \frac{\zeta}{s} \right) (1 - \cos \theta) \quad \rightarrow \quad t_c = -\frac{s}{2} \left(1 - \frac{s_H}{s} \right) (1 - \cos \theta), \quad (144)$$

where s has been kept real to preserve $s = 4E^2$, (E being the c.m.s. energy) and θ is the scattering angle, also real. We add one condition to the mapping $\{I\} \rightarrow \{I_c\}$, that after continuation all the invariants are analytic functions of s_H . It is easily seen that the condition is fulfilled by

$$\bar{k}_2^c = \bar{p} + i\bar{q}, \quad \bar{p} = \frac{1}{2\sqrt{s}} \left(s + \mu_H^2, 0, 0, -s + \mu_H^2 \right), \quad \bar{q} = -\frac{\mu_H \gamma_H}{2\sqrt{s}} (1, 0, 0, 1), \quad (145)$$

i.e. $q^2 = 0$, corresponding to

$$\bar{k}_2^c = \frac{1}{2\sqrt{s}} (s_H + s, 0, 0, s_H - s). \quad (146)$$

In principle there is no need to discuss crossed channels separately. Indeed, any function $A(\{p\})$, after going through complex momenta, may be analytically continued back to the real axis but with negative energies for some of the incoming or outgoing particles. The result of this analytical continuation is the amplitude for a different physical process (e.g. $H \rightarrow ggg$). One should only pay attention to the fact that

$$A(\{I\}) = \langle a|S|b \rangle \quad \bar{A}(\{I\}) = \langle b|S|a \rangle \quad \bar{A}_c(\{I_c\}) \neq A_c^\dagger(\{I_c\}), \quad (147)$$

for complex invariants. Let us consider the decay of a Higgs boson of virtuality $P^2 = \zeta$ into three massless particles of momenta $k_1 \dots k_3$. We define invariants $s_{ij} = (k_i + k_j)^2$ and angles θ_{ij} . Select one invariant, say s_{12} , to remain real and keep θ_{12} also real. The analytic continuation is defined by

$$s_{23}^c = \frac{1}{2} \left[\zeta - s_{12} - \left((\zeta - s_{12})^2 - 4c\zeta s_{12} \right)^{1/2} \right], \quad s_{13}^c = \frac{1}{2} \left[\zeta - s_{12} + \left((\zeta - s_{12})^2 - 4c\zeta s_{12} \right)^{1/2} \right], \quad (148)$$

with $c = \cot^2(\theta_{12}/2)$. Of course, we can keep any of the s_{ij} real and define analytic continuations of the same function, $\Gamma_{H \rightarrow 3}$, in different portions of the 3-dimensional, complex, space s_{12}, s_{13} and s_{23} : in the sense of analytic continuation there is no ambiguity. The choice of which invariant remains real is equivalent to the choice of which momentum is fixed by conservation. To follow the argument we write

$$\begin{aligned} \Gamma_{H \rightarrow 3}(\zeta) &= \frac{1}{2\sqrt{\zeta}} \int d\mathbb{I}_2 \sum_{s,c} \left| A_{H \rightarrow 3}(\{I\}) \right|^2 = \frac{1}{2\sqrt{\zeta}} \int_0^\zeta ds_{12} \int_0^{\zeta - s_{12}} ds_{13} \sum_{s,c} \left| A_{H \rightarrow 3}(\zeta, s_{12}, s_{13}) \right|^2 \\ &= \frac{1}{2\sqrt{\zeta}} \int_0^\zeta ds_{12} \int_{-1}^{+1} d\cos \theta_{12} J(\cos \theta_{12}, s_{12}, \zeta) \Theta \sum_{s,c} \left| A_{H \rightarrow 3}(\zeta, s_{12} \cos \theta_{12}) \right|^2, \end{aligned} \quad (149)$$

where Θ is the condition $(\zeta - s_{12})^2 \geq 4c\zeta s_{12}$,

$$\Gamma_{H \rightarrow 3}(\zeta) = \frac{1}{2\sqrt{\zeta}} \int_{-1}^{+1} d\cos \theta_{12} \int_0^{\zeta_-} ds_{12} J(\cos \theta_{12}, s_{12}, \zeta) \sum_{s,c} \left| A_{H \rightarrow 3}(\zeta, s_{12} \cos \theta_{12}) \right|^2, \quad (150)$$

$$\zeta_- = \left(\cot \frac{\theta_{12}}{2} - \csc \frac{\theta_{12}}{2} \right)^2 \zeta. \quad (151)$$

A more democratic approach in dealing with H decay into n massless states is defined by the following choice:

$$p_i \rightarrow p_i(\lambda, \kappa) = (\lambda + i\kappa) p_i \rightarrow p_i^c = (\alpha + i\beta) p_i, \quad i = 1 \dots n+1 \quad (152)$$

where $p_i^2 = 0$ for $i > 1$ and

$$\alpha^2 - \beta^2 = \frac{\mu_H^2}{p_1^2}, \quad \alpha\beta = -\frac{1}{2} \frac{\mu_H \gamma_H}{p_1^2}. \quad (153)$$

This continuation respects momentum conservation and mass-shell condition for (massless) stable particles and works as long as the continuation passes through analytic regions of the integrand as λ varies from 1 to α and κ varies from 0 to β .

There is never any problem with fully inclusive quantities but a careful discussion is needed if we want to consider differential distributions with cuts: in this case one would like to integrate a function, whose arguments have been analytically continued into the complex plane, over a real (fixed) phase-space. In this case $\Gamma_{H \rightarrow 3}(\zeta)$ becomes

$$\frac{1}{2\sqrt{\zeta}} \int_{-1}^{+1} d\cos\theta_{12} \int_0^{\zeta_-} ds_{12} J(\cos\theta_{12}, s_{12}, \zeta) \sum_{s,c} \left| A_{H \rightarrow 3}(s_H, s_{12} \cos\theta_{12}) \right|^2 \quad (154)$$

To close the discussion we should say that the definition of signal is always conventional since differences (that are non-resonant) will always be included into background plus interference. Furthermore, when main emphasis is on differential distributions in $pp \rightarrow 4f$ there is little meaning in splitting the whole process into components; vice versa, when the problem is with extracting pseudo-observables, e.g. $\Gamma_{H \rightarrow 4f}$, analytic continuation is performed only after integration over all variables but the Higgs virtuality. Nevertheless, if one wants to introduce cuts on differential distributions we have two alternatives. We can define⁶

$$\Gamma_{H \rightarrow 3}(s_H) = \text{Re} \Gamma_{H \rightarrow 3}^c(s_H), \quad (155)$$

$$\Gamma_{H \rightarrow 3}^c(s_H) = \frac{1}{2\sqrt{s_H}} \int_{-1}^{+1} d\cos\theta_{12} \int_{\gamma} ds_{12} J(\cos\theta_{12}, s_{12}, \zeta) \sum_{s,c} \left| A_{H \rightarrow 3}(s_H, s_{12} \cos\theta_{12}) \right|^2 \quad (156)$$

where γ is a curve in the complex s_{12} -plane connecting the origin with the point $s_{12} = s_H^-$ (s_H^- being the continuation of ζ_- from ζ to s_H) provided the integrand is analytic through γ . Finally, we project back into the real s_{12} -axis with a change of variable

$$\int_{\gamma} ds_{12} = \int_0^{\zeta_-} ds_{12} J_c(s_{12}, \zeta, s_H), \quad (157)$$

where J_c is the Jacobian of the transformation.

Alternatively the NLO corrections to a process with $n+1$ external legs can be written as a sum over D , the set of scalar one-loop, $n+1$ -leg diagrams

$$\sum_{s,c} \left| A_{H \rightarrow n}(\{I\}) \right|^2 = \text{Re} \sum_{d \in D} Q_d(\zeta, \{I\}) \int_{S_d} [dx_d] V_d^{-N_d - \varepsilon}(\{x_d\}, \zeta, \{I\}), \quad (158)$$

where Q_d are functions of the invariants, $\{x\}$ are the Feynman parameters that parametrize the loop integral for diagram d , S_d is a simplex in the x -space, V_d is a quadratic(linear) form in the Feynman parameters(invariants) and N_d is a positive integer ($4 - \varepsilon$ is the space-time dimensionality). We can introduce cuts on the real kinematics,

$$\Gamma_{H \rightarrow n}^{\text{cut}}(\zeta) = \frac{1}{2\sqrt{\zeta}} \int dI_{3n-7}^{\text{cut}} \sum_{s,c} \left| A_{H \rightarrow n}(\{I\}) \right|^2, \quad (159)$$

⁶We gratefully acknowledge S. Pozzorini for an important suggestion on this point.

perform first the integration over the phase space with cuts, perform analytic continuation in one variable ($\zeta \rightarrow s_H$) while doing the integration over Feynman parameters (which requires continuation into the second Riemann sheet). The functions Q_d may contain square roots, depending on the masses of the final states and on their number. For massless final states and $n \leq 3$ each Q_d is a rational function of the invariants. For higher values of n it is well-known that phase-space integrals may lead to elliptic functions.

To give an example we consider $H(p) \rightarrow g(k_1) + g(k_2) + g(k_3)$ with $s = (p_1 - k_1)^2$ and $t = (p - k_3)^2$. For instance, there will be a contribution from the direct box with internal top quarks; the fully extrapolated contribution corresponding to $Q = 1$ from Eq.(158) can be cast into the following (manifestly finite) form:

$$\int_0^1 dx \int_0^x dy \left[\text{Li}_2 \left(\frac{r_b - r_a}{1 - r_a} \right) + \text{Li}_2(r_a) - \text{Li}_2(r_b) \right] \frac{1}{(1-x)y(x-y)}, \quad (160)$$

$$r_a = \frac{\zeta}{m_t^2} y(1-x), \quad r_b = \frac{\zeta}{m_t^2} y(1-y). \quad (161)$$

If we impose a cut, e.g. $(1 - z_1)\zeta \leq s \leq (1 - z_2)\zeta$, the result is equally compact,

$$\int_0^1 dx \int_0^x dy \left[\text{Li}_2 \left(z_1 \frac{r_b - r_a}{1 - r_a} \right) + \text{Li}_2 \left(z_1 \frac{r_a}{1 - z_1 r_a} \right) - \text{Li}_2 \left(z_1 \frac{r_b}{1 - z_1 r_a} \right) \right. \\ \left. - \text{Li}_2 \left(z_2 \frac{r_b - r_a}{1 - r_a} \right) - \text{Li}_2 \left(z_2 \frac{r_a}{1 - z_2 r_a} \right) + \text{Li}_2 \left(z_2 \frac{r_b}{1 - z_2 r_a} \right) \right] \frac{1}{(1-x)y(x-y)}. \quad (162)$$

The technique we have described is easily extendible to an arbitrary number of legs. Consider a process $N \rightarrow 0$ with all incoming momenta; a convenient way of describing the boundaries of the phase space, the relations between vectors and invariants and the non-linear constraints that arise when $N \geq 6$ is the following. If p_1 is the momentum associated to the Higgs boson we redefine n-dimensional momenta and introduce components

$$p_1 = (\mu_H, 0_{n-1}), \quad (163)$$

where 0_k is a string of k zero components. Then we introduce

$$(h^N)_{ij} = -p_i \cdot p_j, \quad i, j = 1, \dots, N, \quad (164)$$

$$h_{kl}^N = h^N \quad \text{with row } k \text{ and column } l \text{ removed,} \\ h_{kl;rs}^N = h_{kl}^N \quad \text{with row } r \text{ and column } s \text{ removed,} \quad (165)$$

etc. The vector p_2 is defined by

$$p_2 = \left(\frac{h_{12}^2}{\mu_H}, 0_{n-2}, \sqrt{\frac{\det h^2}{\det h^1}} \right). \quad (166)$$

Next n-dimensional vectors will be

$$p_3 = \left(\frac{h_{13}^3}{\mu_H}, 0_{n-3}, -\frac{\det h_{32}^3}{\sqrt{\det h^1 \det h^2}}, \sqrt{\frac{\det h^3}{\det h^2}} \right), \\ p_4 = \left(\frac{h_{14}^4}{\mu_H}, 0_{n-4}, -\frac{\det h_{43;32}^4}{\sqrt{\det h^1 \det h^2}}, \frac{\det h^{4;43}}{\sqrt{\det h^2 \det h^3}}, \sqrt{\frac{\det h^4}{\det h^3}} \right), \quad (167)$$

etc. If $N = 5$ then momentum conservation gives $p_5 = -\sum p_i$. If, instead $N = 6$, p_6 follows from momentum conservation whereas p_5 requires a fifth component; if $n = 4$ the vanishing of the fifth component requires $\det h^5 = 0$. The boundary of the phase space is determined by the equations

$$\det h^2 < 0, \dots, \det h^{N-1} < 0. \quad (168)$$

As we have mentioned several times the analytic continuation requires knowledge of the branch cuts of the integrand. When the Higgs boson is the only massive external line a box can be expressed in terms of R -functions (see Appendix B of Ref. [90]):

$$R(y_0, y_1) = \int_0^1 dy \frac{1}{y - y_0} \left[\ln(y - y_1) - \ln(y_0 - y_1) \right], \quad (169)$$

where $y_{0,1}$ depend on the invariants of the problem. The function R has the following branch cuts in the complex y_0, y_1 -space:

$$0 \leq x \leq 1 \quad \begin{cases} 1) y_1 = (1-x)y_0 \\ 2) y_1 = (1-x)y_0 + x \\ 3) y_0 = x y_1 \\ 4) y_0 = x y_1 + 1 - x \end{cases}$$

Pentagons etc. are always linear combination of boxes.

C.2 Pseudo-observables

We consider now the problem of extracting pseudo-observables from matrix elements. First we introduce the two-body phase-space,

$$\begin{aligned} \Phi_2(s, s_1, s_2) &= \frac{1}{8\pi^2\sqrt{s}} \int \prod_{i=1,2} d^4 p_i \delta^+(p_i^2 + s_i) \delta^4(P - p_1 - p_2) \\ &= \frac{1}{16\pi\sqrt{s}} \frac{\lambda^{1/2}(s, s_1, s_2)}{s} \theta(s - (\sqrt{s_1} + \sqrt{s_2})^2) \quad s \xrightarrow{\sim} \infty \frac{1}{16\pi\sqrt{s}}, \end{aligned} \quad (170)$$

with $P^2 = -s$. Consider again the process $H(P) \rightarrow Z(p_1) + Z(p_2)$ with an amplitude given by

$$A_{\mu\nu}^0 = -g \frac{M_W}{\cos^2\theta} \delta_{\mu\nu}, \quad A_{\mu\nu}^1 = \frac{g^3}{M_W} \left[s_H F_d \delta_{\mu\nu} + F_p p_{1\nu} p_{2\mu} \right]. \quad (171)$$

The form factors are function of the external invariants and of the internal masses but they are computed at the Higgs complex pole, i.e.

$$F_{d,p} = F_{d,p}(s_H, s_H, M_Z^2, M_Z^2), \quad (172)$$

so that they are gauge parameter independent. We introduce the following quantity:

$$D_2 = \frac{1}{|\Delta_H(s)|^2} \Phi_2(s, M_Z^2, M_Z^2) \left| (A_{\mu\nu}^0 + A_{\mu\nu}^1) e_L^\mu(p_1) e_L^\nu(p_2) \right|^2, \quad (173)$$

which is the product of a Higgs propagator times the S -matrix element for the Higgs boson into a pair of longitudinal Z bosons. We obtain

$$\begin{aligned} D_2 &= \frac{1}{|\Delta_H(s)|^2} \Gamma_{H \rightarrow Z_L Z_L}(s), \\ \Gamma_{H \rightarrow Z_L Z_L}(s) &= \frac{g^2}{16\pi\sqrt{s}} \frac{\lambda^{1/2}(s, M_Z^2, M_Z^2)}{s} \left(\Gamma_0 + \frac{g^2}{\cos^2\theta} \text{Re}\Gamma_1 \right), \end{aligned} \quad (174)$$

$$\Gamma_0 = \frac{M_Z^2}{\cos^2\theta} + \frac{1}{4} \frac{\lambda(s, M_Z^2, M_Z^2)}{M_Z^2 \cos^2\theta}, \quad \Gamma_1 = \frac{1}{4} \frac{s - M_Z^2}{M_Z^4} \lambda(s, M_Z^2, M_Z^2) F_p - \frac{s_H}{2} \left[4 + \frac{\lambda(s, M_Z^2, M_Z^2)}{M_Z^4} \right] F_d. \quad (175)$$

There is no problem with gauge parameter dependence in Eq.(175); nevertheless, it is useful to separate the residue of the Higgs complex pole and also to introduce Z complex poles obtaining a pseudo-observable

$$\Gamma_{H^c \rightarrow Z_L^c Z_L^c} = \frac{g^2}{16\pi\sqrt{|s_H|}} \text{Re} \left(\bar{\Gamma}_0 + \frac{g^2}{\cos^2\theta} \bar{\Gamma}_1 \right), \quad |s_H| \gg |s_Z|, \quad (176)$$

where $\bar{\Gamma}$ is obtained with the substitution $s \rightarrow s_H$ and $M_Z^2 \rightarrow s_Z$ in Γ . As a second step we consider $H \rightarrow ZZ \rightarrow e^+e^-\mu^+\mu^-$ and define

$$D_4 = \frac{1}{|\Delta_H(s)|^2} \sum_{\text{spins}} \Phi_4 \left| (A_{\mu\nu}^0 + A_{\mu\nu}^1) J^\mu J^\nu \right|^2 \frac{1}{|\Delta_Z(s_1)|^2 |\Delta_Z(s_2)|^2}, \quad (177)$$

where J is the (conserved) leptonic current and

$$\Phi_4 = \frac{1}{(2\pi)^8} \frac{1}{2\sqrt{s}} \int \prod_{i=1,2} d^4 q_i d^4 k_i \delta^+(q_i^2) \delta^+(k_i^2) \delta^4 \left(P - \sum_i (q_i + k_i) \right), \quad (178)$$

is the phase-space for $H \rightarrow$ leptons. We write it as

$$\begin{aligned} \Phi_4 &= \frac{1}{(2\pi)^8} \frac{1}{2\sqrt{s}} \int d^4 p_1 d^4 p_2 \delta^4(P - p_1 - p_2) \int \prod_{i=1,2} d^4 q_i d^4 k_i \delta^+(q_i^2) \delta^+(k_i^2) \\ &\quad \times \delta^4(p_1 - q_1 - k_1) \delta^4(p_2 - q_2 - k_2) \\ &= \frac{\sqrt{s_1 s_2}}{\pi^2} \int ds_1 ds_2 \Phi_2(s, s_1, s_2) \Phi_2(s_1, 0, 0) \Phi_2(s_2, 0, 0). \end{aligned} \quad (179)$$

The form factors $F_{d,p}$ are computed with $s = s_H$ and $s_{1,2} = s_Z$ to guarantee gauge parameter independence. Based on longitudinal polarization dominance (see Appendix B) for $s \rightarrow \infty$ we introduce longitudinal polarization vectors in the numerator of the Z-propagators and obtain

$$\sum_{\text{spins}} \left| (A_{\mu\nu}^0 + A_{\mu\nu}^1) J^\mu J^\nu \right|^2 = \sum_{\text{spins}} \left| J \cdot e_L(p_1) \right|^2 \left| J \cdot e_L(p_2) \right|^2 g^2 \text{Re } \mathcal{A}, \quad (180)$$

$$\mathcal{A} = \frac{s_Z}{\cos^2 \theta} + \frac{g^2}{\cos^2 \theta} \left\{ \frac{1}{4} \frac{s - s_1 - s_2}{s_1 s_2} \lambda(s, s_1, s_2) F_p - \frac{1}{2} \frac{s_H}{s_1 s_2} \left[\lambda(s, s_1, s_2) + 4 s_1 s_2 \right] F_d \right\}. \quad (181)$$

Therefore, taking the residue of all complex poles, in the limit $|s_H| \rightarrow \infty$ we obtain

$$\frac{d^2 D_4}{ds_1 ds_2} = \frac{|s_Z|}{\pi^2} \frac{1}{|\Delta_H(s)|^2} \frac{\Gamma_{Z^c \rightarrow e^+e^-}}{|\Delta_Z(s_1)|^2} \frac{\Gamma_{Z^c \rightarrow \mu^+\mu^-}}{|\Delta_Z(s_2)|^2} \Gamma_{H^c \rightarrow Z_L^c Z_L^c} + \text{non-resonant terms}. \quad (182)$$

For an Heavy Higgs boson is straightforward to extract the pseudo-observable defining $H \rightarrow Z_L Z_L$ from the decay H into two pairs of leptons of different flavor. Interference effects, as well as transverse polarizations, will be analyzed in a subsequent paper.

References

- [1] LHC Higgs Cross Section Working Group Collaboration, S. Dittmaier et al., *Handbook of LHC Higgs Cross Sections: 1. Inclusive Observables*, arXiv:1101.0593 [hep-ph].
- [2] S. Dittmaier, S. Dittmaier, C. Mariotti, G. Passarino, R. Tanaka, et al., *Handbook of LHC Higgs Cross Sections: 2. Differential Distributions*, arXiv:1201.3084 [hep-ph]. Report of the LHC Higgs Cross Section Working Group.
- [3] S. Actis, G. Passarino, C. Sturm, and S. Uccirati, *Two-loop threshold singularities, unstable particles and complex masses*, Phys. Lett. **B669** (2008) 62–68, arXiv:0809.1302 [hep-ph].
- [4] G. Passarino, C. Sturm, and S. Uccirati, *Higgs pseudo-observables, second Riemann sheet and all that*, Nucl. Phys. **B834** (2010) 77–115, arXiv:1001.3360 [hep-ph].
- [5] J. Ellis, J. Espinosa, G. Giudice, A. Hoecker, and A. Riotto, *The Probable Fate of the Standard Model*, Phys.Lett. **B679** (2009) 369–375, arXiv:0906.0954 [hep-ph].
- [6] ATLAS Collaboration Collaboration, G. Aad et al., *Search for a heavy Standard Model Higgs boson in the channel $H \rightarrow ZZ \rightarrow llqq$ using the ATLAS detector*, Phys.Lett. **B707** (2012) 27–45, arXiv:1108.5064 [hep-ex].
- [7] A. Collaboration, *Search for the Standard Model Higgs boson in the decay channel $H \rightarrow ZZ^* \rightarrow 4l$ with 4.8 fb^{-1} of pp collisions at $\sqrt{s} = 7 \text{ TeV}$ with ATLAS*, arXiv:1202.1415 [hep-ex].
- [8] A. Collaboration, *Search for the Standard Model Higgs boson in the diphoton decay channel with 4.9 fb^{-1} of pp collisions at $\sqrt{s} = 7 \text{ TeV}$ with ATLAS*, arXiv:1202.1414 [hep-ex].
- [9] A. Collaboration, *Combined search for the Standard Model Higgs boson using up to 4.9 fb^{-1} of pp collision data at $\sqrt{s} = 7 \text{ TeV}$ with the ATLAS detector at the LHC*, arXiv:1202.1408 [hep-ex].
- [10] A. Graziano and f. t. C. Collaboration, *Analysis strategy for the SM Higgs boson search in the four-lepton final state in CMS*, arXiv:1202.1746 [hep-ex].
- [11] CMS Collaboration Collaboration, S. Chatrchyan et al., *Search for the standard model Higgs boson in the H to ZZ to $2l 2\nu$ channel in pp collisions at $\sqrt{s} = 7 \text{ TeV}$* , arXiv:1202.3478 [hep-ex].
- [12] CMS Collaboration Collaboration, S. Chatrchyan et al., *Search for the standard model Higgs boson in the H to ZZ to $ll \tau \tau$ decay channel in pp collisions at $\sqrt{s} = 7 \text{ TeV}$* , arXiv:1202.3617 [hep-ex].
- [13] S. Kanemura, Y. Okada, H. Taniguchi, and K. Tsumura, *Indirect bounds on heavy scalar masses of the two-Higgs-doublet model in light of recent Higgs boson searches*, Phys.Lett. **B704** (2011) 303–307, arXiv:1108.3297 [hep-ph].
- [14] Y. Bai, J. Fan, and J. L. Hewett, *Hiding a Heavy Higgs Boson at the 7 TeV LHC*, arXiv:1112.1964 [hep-ph].
- [15] G. Passarino, C. Sturm, and S. Uccirati, *Complete Electroweak Corrections to Higgs production in a Standard Model with four generations at the LHC*, Phys.Lett. **B706** (2011) 195–199, arXiv:1108.2025 [hep-ph].
- [16] A. Denner, S. Dittmaier, A. Muck, G. Passarino, M. Spira, et al., *Higgs production and decay with a fourth Standard-Model-like fermion generation*, arXiv:1111.6395 [hep-ph].
- [17] M. E. Peskin and J. D. Wells, *How can a heavy Higgs boson be consistent with the precision electroweak measurements?*, Phys.Rev. **D64** (2001) 093003, arXiv:hep-ph/0101342 [hep-ph].
- [18] A. Ghinculov and T. Binoth, *On the position of a heavy Higgs pole*, Phys.Lett. **B394** (1997) 139–146, arXiv:hep-ph/9611357 [hep-ph].

- [19] A. Ghinculov and J. van der Bij, *The Higgs resonance shape in gluon fusion: Heavy Higgs effects*, Nucl.Phys. **B482** (1996) 59–72, [arXiv:hep-ph/9511414](#) [hep-ph].
- [20] A. Ghinculov, *Two loop heavy Higgs correction to Higgs decay into vector bosons*, Nucl. Phys. **B455** (1995) 21–38, [arXiv:hep-ph/9507240](#) [hep-ph].
- [21] C. Anastasiou, S. Buhler, F. Herzog, and A. Lazopoulos, *Total cross-section for Higgs boson hadroproduction with anomalous Standard Model interactions*, [arXiv:1107.0683](#) [hep-ph].
- [22] C. Anastasiou, S. Buehler, F. Herzog, and A. Lazopoulos, *Inclusive Higgs boson cross-section for the LHC at 8 TeV*, [arXiv:1202.3638](#) [hep-ph].
- [23] M. J. G. Veltman, *Unitarity and causality in a renormalizable field theory with unstable particles*, Physica **29** (1963) 186–207.
- [24] R. Jacob and R. Sachs, *Mass and Lifetime of Unstable Particles*, Phys.Rev. **121** (1961) 350–356.
- [25] G. Valent, *Renormalization and second sheet poles in unstable particle theory*, Nucl.Phys. **B65** (1973) 445–459.
- [26] J. Lukierski, *Field operator for unstable particle and complex mass description in local QFT*, Fortsch.Phys. **28** (1980) 259.
- [27] C. Bollini and L. Oxman, *Unitarity and complex mass fields*, Int.J.Mod.Phys. **A8** (1993) 3185–3198.
- [28] P. A. Grassi, B. A. Kniehl, and A. Sirlin, *Width and partial widths of unstable particles in the light of the Nielsen identities*, Phys.Rev. **D65** (2002) 085001, [arXiv:hep-ph/0109228](#) [hep-ph].
- [29] P. A. Grassi, B. A. Kniehl, and A. Sirlin, *Width and partial widths of unstable particles*, Phys. Rev. Lett. **86** (2001) 389–392, [arXiv:hep-th/0005149](#).
- [30] B. A. Kniehl and A. Sirlin, *Mass and width of a heavy Higgs boson*, Phys.Lett. **B440** (1998) 136–140, [arXiv:hep-ph/9807545](#) [hep-ph].
- [31] B. A. Kniehl and A. Sirlin, *Differences between the pole and on-shell masses and widths of the Higgs boson*, Phys.Rev.Lett. **81** (1998) 1373–1376, [arXiv:hep-ph/9805390](#) [hep-ph].
- [32] R. G. Stuart, *Gauge invariance, analyticity and physical observables at the Z0 resonance*, Phys.Lett. **B262** (1991) 113–119.
- [33] E. N. Argyres, W. Beenakker, G. J. van Oldenborgh, A. Denner, S. Dittmaier, et al., *Stable calculations for unstable particles: Restoring gauge invariance*, Phys.Lett. **B358** (1995) 339–346, [arXiv:hep-ph/9507216](#) [hep-ph].
- [34] W. Beenakker, G. J. van Oldenborgh, A. Denner, S. Dittmaier, J. Hoogland, et al., *The Fermion loop scheme for finite width effects in e^+e^- annihilation into four fermions*, Nucl.Phys. **B500** (1997) 255–298, [arXiv:hep-ph/9612260](#) [hep-ph].
- [35] F. Jegerlehner, M. Y. Kalmykov, and O. Veretin, *MS-bar versus pole masses of gauge bosons. 2. Two loop electroweak fermion corrections*, Nucl.Phys. **B658** (2003) 49–112, [arXiv:hep-ph/0212319](#) [hep-ph].
- [36] F. Jegerlehner, M. Kalmykov, and O. Veretin, *MS versus pole masses of gauge bosons: Electroweak bosonic two loop corrections*, Nucl.Phys. **B641** (2002) 285–326, [arXiv:hep-ph/0105304](#) [hep-ph].
- [37] M. Beneke, A. Chapovsky, A. Signer, and G. Zanderighi, *Effective theory calculation of resonant high-energy scattering*, Nucl.Phys. **B686** (2004) 205–247, [arXiv:hep-ph/0401002](#) [hep-ph].

- [38] M. Beneke, A. Chapovsky, A. Signer, and G. Zanderighi, *Effective theory approach to unstable particle production*, Phys.Rev.Lett. **93** (2004) 011602, arXiv:hep-ph/0312331 [hep-ph]. 4 pages, 1 figure Report-no: PITHA 03/13, IPPP/03/82, FERMILAB-Pub-03/407-T.
- [39] J. Lukierski and M. Oziewicz, *Lee model with v -particle having continuous spectrum of asymptotic masses*, Acta Phys.Polon. **B3** (1972) 231–246.
- [40] A. Denner, S. Dittmaier, M. Roth, and L. Wieders, *Electroweak corrections to charged-current $e^+e^- \rightarrow 4$ fermion processes: Technical details and further results*, Nucl. Phys. **B724** (2005) 247–294, arXiv:hep-ph/0505042 [hep-ph].
- [41] A. Denner and S. Dittmaier, *The complex-mass scheme for perturbative calculations with unstable particles*, Nucl. Phys. Proc. Suppl. **160** (2006) 22–26, arXiv:hep-ph/0605312.
- [42] G. Passarino, *Single W production and fermion-loop scheme: Numerical results*, Nucl. Phys. **B578** (2000) 3–26, arXiv:hep-ph/0001212.
- [43] S. Actis and G. Passarino, *Two-loop renormalization in the standard model. III: Renormalization equations and their solutions*, Nucl. Phys. **B777** (2007) 100–156, arXiv:hep-ph/0612124.
- [44] S. Actis and G. Passarino, *Two-Loop Renormalization in the Standard Model Part II: Renormalization Procedures and Computational Techniques*, Nucl.Phys. **B777** (2007) 35–99, arXiv:hep-ph/0612123 [hep-ph].
- [45] G. Passarino, *$W W$ scattering and perturbative unitarity*, Nucl.Phys. **B343** (1990) 31–59.
- [46] G. Passarino, *Large Masses, Unitarity and One Loop Corrections*, Phys. Lett. **B156** (1985) 231.
- [47] A. Bredenstein, A. Denner, S. Dittmaier, A. Mück, and M. M. Weber, *Prophecy4f: A Monte Carlo generator for a proper description of the Higgs decay into 4 fermions*, [Http://omnibus.uni-freiburg.de/sd565/programs/prophecy4f/prophecy4f.html](http://omnibus.uni-freiburg.de/sd565/programs/prophecy4f/prophecy4f.html), 2010.
- [48] T. Binoth, M. Ciccolini, N. Kauer, and M. Kramer, *Gluon-induced W -boson pair production at the LHC*, JHEP **0612** (2006) 046, arXiv:hep-ph/0611170 [hep-ph].
- [49] J. M. Campbell, R. Ellis, and C. Williams, *Gluon-Gluon Contributions to $W^+ W^-$ Production and Higgs Interference Effects*, JHEP **1110** (2011) 005, arXiv:1107.5569 [hep-ph].
- [50] N. Kauer, *Signal-background interference in $gg \rightarrow H \rightarrow VV$* , arXiv:1201.1667 [hep-ph].
- [51] M. Spira, A. Djouadi, D. Graudenz, and P. M. Zerwas, *Higgs boson production at the LHC*, Nucl. Phys. **B453** (1995) 17–82, hep-ph/9504378.
- [52] H. Weldon, *The Description of Unstable Particles in Quantum Field Theory*, Phys.Rev. **D14** (1976) 2030.
- [53] H. Lehmann, K. Symanzik, and W. Zimmermann, *On the formulation of quantized field theories. II*, Nuovo Cim. **6** (1957) 319–333.
- [54] J. C. Collins, D. E. Soper, and G. F. Sterman, *Factorization of Hard Processes in QCD*, Adv.Ser.Direct.High Energy Phys. **5** (1988) 1–91, arXiv:hep-ph/0409313 [hep-ph]. To be publ. in 'Perturbative QCD' (A.H. Mueller, ed.) (World Scientific Publ., 1989).
- [55] S. Alioli, P. Nason, C. Oleari, and E. Re, *NLO Higgs boson production via gluon fusion matched with shower in POWHEG*, JHEP **04** (2009) 002, arXiv:0812.0578 [hep-ph].
- [56] C. Schwinn, *Consistent Dyson summation of Higgs propagators in nonlinear parameterizations revisited*, Eur.Phys.J. **C38** (2004) 335–348, arXiv:hep-ph/0407053 [hep-ph]. 14 pages, LaTeX (feynmf.sty included): references and clarifying remarks added: published version Report-no: MZ-TH/04-06 Journal-ref: Eur.Phys.J. C38 (2004) 335 - 348 DOI: 10.1140/epjc/s2004-02057-2.

- [57] M. H. Seymour, *The Higgs boson line shape and perturbative unitarity*, Phys.Lett. **B354** (1995) 409–414, arXiv:hep-ph/9505211 [hep-ph].
- [58] E. Glover and J. van der Bij, *Z Boson Pair Production via Gluon Fusion*, Nucl.Phys. **B321** (1989) 561.
- [59] G. Valencia and S. Willenbrock, *The Heavy Higgs resonance*, Phys.Rev. **D46** (1992) 2247–2251.
- [60] M. W. Grunewald, G. Passarino, E. Accomando, A. Ballestrero, P. Bambade, et al., *Reports of the Working Groups on Precision Calculations for LEP2 Physics: Proceedings. Four fermion production in electron positron collisions*, arXiv:hep-ph/0005309 [hep-ph].
- [61] P. Gambino and P. A. Grassi, *The Nielsen identities of the SM and the definition of mass*, Phys.Rev. **D62** (2000) 076002, arXiv:hep-ph/9907254 [hep-ph].
- [62] M. Veltman, *Generalized ward identities and yang-mills fields*, Nucl.Phys. **B21** (1970) 288–302.
- [63] J. Taylor, *Ward Identities and Charge Renormalization of the Yang-Mills Field*, Nucl.Phys. **B33** (1971) 436–444.
- [64] A. Slavnov, *Ward Identities in Gauge Theories*, Theor.Math.Phys. **10** (1972) 99–107.
- [65] D. de Florian and M. Grazzini, *Higgs production through gluon fusion: updated cross sections at the Tevatron and the LHC*, Phys. Lett. **B674** (2009) 291–294, arXiv:0901.2427 [hep-ph].
- [66] M. Grazzini, *NNLO predictions for the Higgs boson signal in the $H \rightarrow WW \rightarrow l\nu l\nu$ and $H \rightarrow ZZ \rightarrow 4l$ decay channels*, arXiv:0801.3232 [hep-ph].
- [67] S. Catani, D. de Florian, and M. Grazzini, *Higgs production in hadron collisions: Soft and virtual QCD corrections at NNLO*, JHEP **05** (2001) 025, arXiv:hep-ph/0102227.
- [68] G. Montagna, O. Nicrosini, F. Piccinini, and G. Passarino, *TOPAZ0 4.0: A new version of a computer program for evaluation of de-convoluted and realistic observables at LEP 1 and LEP 2*, Comput. Phys. Commun. **117** (1999) 278–289, arXiv:hep-ph/9804211.
- [69] A. D. Martin, W. J. Stirling, R. S. Thorne, and G. Watt, *Parton distributions for the LHC*, Eur. Phys. J. **C63** (2009) 189–285, arXiv:0901.0002 [hep-ph].
- [70] B. A. Kniehl and A. Sirlin, *Pole Mass, Width, and Propagators of Unstable Fermions*, Phys.Rev. **D77** (2008) 116012, arXiv:0801.0669 [hep-th].
- [71] HXSWG, *Results at 8 TeV*, [Urlhttps://twiki.cern.ch/twiki/bin/view/LHCPhysics/CERNYellowReportPageAt8TeV](https://twiki.cern.ch/twiki/bin/view/LHCPhysics/CERNYellowReportPageAt8TeV), 2012.
- [72] M. Cacciari and N. Houdeau, *Meaningful characterisation of perturbative theoretical uncertainties*, JHEP **1109** (2011) 039, arXiv:1105.5152 [hep-ph].
- [73] ATLAS Collaboration Collaboration, G. Aad et al., *Search for the Higgs boson in the $H \rightarrow WW(*) \rightarrow l\nu l\nu$ decay channel in pp collisions at $\sqrt{s} = 7$ TeV with the ATLAS detector*, arXiv:1112.2577 [hep-ex].
- [74] A. Frink, B. A. Kniehl, D. Kreimer, and K. Riesselmann, *Heavy Higgs lifetime at two loops*, Phys. Rev. **D54** (1996) 4548–4560, arXiv:hep-ph/9606310 [hep-ph].
- [75] S. Dawson, *Radiative corrections to Higgs boson production*, Nucl. Phys. **B359** (1991) 283–300.
- [76] A. Djouadi, M. Spira, and P. M. Zerwas, *Production of Higgs bosons in proton colliders: QCD corrections*, Phys. Lett. **B264** (1991) 440–446.

- [77] M. Krämer, E. Laenen, and M. Spira, *Soft gluon radiation in Higgs boson production at the LHC*, Nucl. Phys. **B511** (1998) 523–549, [arXiv:hep-ph/9611272](#) [hep-ph].
- [78] R. V. Harlander and W. B. Kilgore, *Soft and virtual corrections to $pp \rightarrow H+X$ at NNLO*, Phys. Rev. **D64** (2001) 013015, [arXiv:hep-ph/0102241](#).
- [79] C. Anastasiou and K. Melnikov, *Higgs boson production at hadron colliders in NNLO QCD*, Nucl. Phys. **B646** (2002) 220–256, [arXiv:hep-ph/0207004](#).
- [80] V. Ravindran, J. Smith, and W. L. Van Neerven, *Next-to-leading order QCD corrections to differential distributions of Higgs boson production in hadron hadron collisions*, Nucl. Phys. **B634** (2002) 247–290, [hep-ph/0201114](#).
- [81] S. Catani, D. de Florian, M. Grazzini, and P. Nason, *Soft-gluon resummation for Higgs boson production at hadron colliders*, JHEP **07** (2003) 028, [hep-ph/0306211](#).
- [82] S. Actis, G. Passarino, C. Sturm, and S. Uccirati, *NLO electroweak corrections to Higgs boson production at hadron colliders*, Phys. Lett. **B670** (2008) 12–17, [arXiv:0809.1301](#) [hep-ph].
- [83] S. Actis, G. Passarino, C. Sturm, and S. Uccirati, *NNLO computational techniques: the cases $H \rightarrow \gamma\gamma$ and $H \rightarrow gg$* , Nucl. Phys. **B811** (2009) 182–273, [arXiv:0809.3667](#) [hep-ph].
- [84] A. Bredenstein, A. Denner, S. Dittmaier, and M. M. Weber, *Precision calculations for $H \rightarrow WW/ZZ \rightarrow 4\text{fermions}$ with PROPHECY4f*, [arXiv:0708.4123](#) [hep-ph].
- [85] J. Bagger and C. Schmidt, *Equivalence Theorem Redux*, Phys.Rev. **D41** (1990) 264.
- [86] G. Passarino, *Indirect measurement of vector boson scattering at high-energies*, Phys.Lett. **B183** (1987) 375.
- [87] G. Passarino, *Covariant polarization bases for spin 1/2, spin 1, spin 3/2 particles and their use*, Nucl.Phys. **B237** (1984) 249.
- [88] G. Passarino, *Helicity Formalism for Transition Amplitudes*, Phys.Rev. **D28** (1983) 2867.
- [89] A. Denner, S. Dittmaier, M. Roth, and D. Wackerroth, *Electroweak radiative corrections to $e^+e^- \rightarrow WW \rightarrow 4\text{ fermions}$ in double pole approximation: The RACOONWW approach*, Nucl.Phys. **B587** (2000) 67–117, [arXiv:hep-ph/0006307](#) [hep-ph].
- [90] G. 't Hooft and M. J. G. Veltman, *Scalar one loop integrals*, Nucl. Phys. **B153** (1979) 365–401.